Metformin improves high-fat diet-induced insulin resistance in mice by downregulating the expression of long noncoding RNA NONMMUT031874.2

ZHI-MEI ZHANG[1,2], ZHI-HONG LIU[1,3], QIAN NIE[1,4], XUE-MEI ZHANG[1,4], LI-QUN YANG[1,2], CHAO WANG[4], LIN-LIN YANG[4] and GUANG-YAO SONG[1,4]

[1]Department of Internal Medicine, Hebei Medical University, Shijiazhuang, Hebei 050017; [2]Department of Endocrinology, Hebei General Hospital; [3]Department of Endocrinology, The Second Hospital of Hebei Medical University; [4]Hebei Key Laboratory of Metabolic Diseases, Hebei General Hospital, Shijiazhuang, Hebei 050051, P.R. China

Received November 27, 2020; Accepted December 30, 2021

DOI: 10.3892/etm.2022.11261

Abstract. Metformin (MET) is the first-line therapeutic option for patients with type 2 diabetes that has garnered substantial attention over recent years. However, an insufficient number of studies have been performed to assess its effects on insulin resistance and the expression profile of long noncoding RNAs (lncRNAs). The present study divided mice into three groups: Control group, high-fat diet (HFD) group and HFD + MET group. A high-throughput sequencing analysis was conducted to detect lncRNA and mRNA expression levels, and differentially expressed lncRNAs were selected. Subsequently, the differentially expressed lncRNAs were validated both *in vivo* and *in vitro* (mouse liver AML12 cells treated with Palmitic acid) models of insulin resistance. After validating randomly selected lncRNAs via reverse transcription-quantitative PCR a novel lncRNA, NONMMUT031874.2, was identified, which was upregulated in the HFD group and reversed with MET treatment. To investigate the downstream mechanism of NONMMUT031874.2, lncRNA-microRNA (miR/miRNA)-mRNA co-expression network was constructed and NONCODE, miRBase and TargetScan databases were used, which indicated that NONMMUT031874.2 may regulate suppressor of cytokine signaling 3 by miR-7054-5p. For the *in vitro* part of the present study, AML12 cells were transfected with small interfering RNA to knock down NONMMUT031874.2 expression before being treated with palmitic acid (PA) and MET. The results showed that the expression of NONMMUT031874.2 was significantly increased whereas miR-7054-5p expression was significantly decreased by PA treatment. By contrast, after knocking down NONMMUT031874.2 expression or treatment with MET, the aforementioned *in vitro* observations were reversed. In addition, it was also found that NONMMUT031874.2 knockdown and treatment with MET exerted similar effects in alleviating insulin resistance and whilst decreasing glucose concentration in AML12 cells. These results suggest that MET treatment can ameliorate insulin resistance by downregulating NONMMUT031874.2 expression.

Introduction

Over the past decade, the incidence of type 2 diabetes has been increasing rapidly (1). Studies have shown that the number of adults suffering from diabetes worldwide in 2015 was ~425 million. If this trend continues, by 2040, the number will reach 629 million (2). Although a wide variety factors can influence the onset of this disease, insulin resistance is wide accepted to be the leading cause (3). Long non-coding RNAs (lncRNAs) are a type of non-coding RNAs that are >200 nucleotides in length and account for 80% of all non-coding RNAs (4). The majority of lncRNAs are conserved and expressed at lower levels than mRNAs (5). Previous studies have reported that lncRNAs in combination with microRNAs (miR or miRNA), mRNAs or proteins can coordinate to regulate gene expression and serve an important role in insulin resistance in humans (6,7). In addition, lncRNAs have been shown to be potential novel biomarkers and therapeutic targets. LncRNA maternally expressed gene 3 (MEG3) is involved in gluconeogenesis. However, lncRNA metastasis associated lung adenocarcinoma transcript 1 (MALAT1) can even affect the insulin signaling pathway and correlate with hepatic *de novo* lipogenesis (8).

Metformin (MET) is a first-line therapeutic option for newly diagnosed patients with type 2 diabetes (9). It functions by suppressing liver gluconeogenesis, which in turn decreases blood glucose levels (10). Studies have previously documented that in rats and cells insulin resistance models, MET can effectively improve insulin resistance via the p53/RAP2A pathway (11). In addition, MET can also alleviate

Correspondence to: Professor Guang-Yao Song, Department of Internal Medicine, Hebei Medical University, 361 Zhongshan East Road, Shijiazhuang, Hebei 050017, P.R. China
E-mail: sguangyao2@163.com

Key words: metformin, lncRNA, high-throughput sequencing, insulin resistance, mice

lipid composition in adipose tissues of diet-induced insulin resistant rats (12). In addition, Wang *et al* revealed that MET can inhibit gluconeogenesis of primary mouse hepatocytes by upregulating lncRNA NR_027710 and downregulating lncRNA ENSMUST00000138573 (13). However, the potential mechanism of lncRNAs in the effects of MET on hepatic insulin resistance remains poorly understood. In addition, it remains unknown if MET can exert changes in the expression of lncRNAs on hepatic insulin resistance. Therefore, in the present study, C57BL/6J mice were fed with high-fat diet to establish insulin resistance model and treatment with MET. A high-throughput sequencing analysis was conducted and AML12 cells were treated with PA to establish insulin resistance model *in vitro*. Subsequently, the effects of MET on lncRNA expression and the mechanism of MET in improving hepatic insulin resistance by regulating lncRNA were investigated.

Materials and methods

In vivo animal models. A total of 42 6-week-old (weight, 22.4±0.6 g) male C57BL/6J mice from Beijing Vital River Laboratory Animal Technology Co., Ltd. [license no. SCXK(Jing)2016-0011]. They were kept in the Clinical Research Center of Hebei General Hospital (Shijiazhuang, China) at a temperature of 23-25˚C and relative humidity of ~60% with a 12-h light/dark cycle. All mice had free access to food and water. This experiment was approved by the Ethics Committee of Hebei General Hospital and complied with the Animal (Scientific Procedures) Act 1986 and associated guidelines (14).

After 1 week of adaptive feeding, the 42 C57BL/6J mice were randomly divided into two groups. In total, 14 mice were assigned into the control group (CON), which were fed with a regular diet (D12450J formula, consisting of 20% protein, 70% carbohydrate, 10% fat and 3.85 kcal/g). By contrast, 28 mice were assigned into the high-fat diet (HFD) group (D12492 formula, consisting of 20% protein, 20% carbohydrate, 60% fat and 5.24 kcal/g) (15). All feed was purchased from Beijing Huafukang Biotechnology Co, Ltd. Body weight and food intake were recorded weekly [food intake (kcal/day)=the total food intake of mice in each group weekly (g) x food calories (kcal/g)/(the number of mice in each group x7 days)]. After 8 weeks of feeding, blood was collected from the tail vein at 0, 15, 30, 60 and 120 min after intraperitoneal glucose injection for the intraperitoneal glucose tolerance test (IPGTT). Area under the curve (AUC) was calculated to compare glucose tolerance between the two groups, which was the sum of the four trapezoidal areas under the curve (the side length is the blood glucose value at different time points, the height is the time of IPGTT and the AUC value is the sum of the four trapezoidal areas under the curve). The insulin sensitivity method developed by Katz *et al* (16) was used, which defined the quantitative insulin sensitivity check index (QUICKI) as $1/[\log (I_0) + \log(G_0)]$, where I_0 is the fasting insulin level and G_0 is the fasting glucose level.

Among the 28 mice in the HFD group, 14 mice were randomly assigned into the HFD + MET group. A MET (Sangon Biotech Co., Ltd.) stock solution was prepared by first mixing 200 mg MET with 1 ml of triple-distilled water, which was then diluted with 0.9% NaCl. Mice in the HFD + MET group were given 200 mg/kg MET daily by oral gavage for 6 weeks (17), whereas mice in the CON and HFD groups were given the same volume of 0.9% NaCl for 6 weeks.

Collection of serum and tissue specimens. After 6 weeks of MET intervention, three mice in each group were randomly selected before an intraperitoneal injection of 1.5 U/40 g insulin (Sigma-Aldrich; Merck KGaA). The mice were then anesthetized by an intraperitoneal injection of 2% sodium pentobarbital (45 mg/kg). After the eyeballs were removed and blood samples were collected, the animals were sacrificed by dislocating the cervical vertebrae under anesthesia. The liver was then quickly removed, snap frozen in liquid nitrogen and stored at -80˚C. The blood samples were centrifuged at 5,000 x g for 15 min at 4˚C before the serum was stored at -80˚C.

Determination of blood indicators. Detection kits for triglyceride (TG; cat. no. A110-1-1), total cholesterol (TC; cat. no. A111-1-1), high-density-lipoprotein cholesterol (HDL-C; cat. no. A112-1-1), free fatty acid (FFA; cat. no. A042-2-1) and low-density-lipoprotein cholesterol (LDL-C; cat. no. A113-1-1) were purchased from Nanjing Jiancheng Bioengineering Institute. An insulin chemiluminescence ELISA kit (cat. no. H203-1-2; ALPCO) was used to measure the levels of serum insulin. All procedures were performed in accordance with the manufacturers' protocols.

Establishment of in vitro models and transfections

Preparation of the transfection complex. In total, three siRNA sequences (NONMMUT031874.2-1368 sense, 5'-CCUGUAGACCACUUGGAAATT-3', and antisense, 5'UUUCCAAGUGGUCUACAGGTT-3'; NONMMUT031874.2-1502 sense, 5'-GCAGUGUGUCUACUGUAUUTT-3', and antisense 5'-AAUACAGUAGACACACUGCTT-3'; NONMMUT031874.2-1739 sense, 5'-GCAGGAGCUUUGCAGCAUATT-3', and antisense 5'-UAUGCUGCAAAGCUCCUGCTT-3') and siRNA-NONMMUT031874.2 negative control sequence (sense, 5'-UUCUCCGAACGUGUCACGUTT-3', and antisense, 5'-ACGUGACACGUUCGGAGAATT-3') were purchased from Suzhou GenePharma Co., Ltd. Transfection was performed when the cells were at ~60% confluency. DEPC water (125 μl) was added to each siRNA to prepare a RNA oligo stock solution of 20 μM, which was stored at -20˚C. In total, 200 μl Opti-MEM (Thermo Fisher Scientific, Inc.), 5 μl RNA oligo stock solution and 10 μl siRNA-Mate transfection reagent (Suzhou GenePharma Co., Ltd.) were used to prepare the transfection complex at room temperature. Once the transfection complex was formed, it was added to the cells immediately.

Establishment of cell model and cell viability assay. A mouse hepatic cell line AML12 was purchased from The Cell Bank of Type Culture Collection of the Chinese Academy of Sciences. These cells were cultured at 37˚C under 5% CO_2 with DMEM/F-12 medium (Gibco; Thermo Fisher Scientific, Inc.) supplemented with 10% FBS (Gibco; Thermo Fisher Scientific, Inc.), 1X insulin-transferrin-selenium (Sigma-Aldrich; Merck KGaA) and 40 ng/ml dexamethasone (Sigma-Aldrich; Merck KGaA).

To establish the insulin resistance model, 0.25 mM palmitic acid (PA; Sigma-Aldrich; Merck KGaA) at room temperature was added to the DMEM/F-12 medium (18), before the glucose

concentration in the medium was determined at 0, 8, 16 and 24 h using a glucose oxidase assay kit (Applygen Technologies, Inc.) to assess establishment of the insulin resistance model. After cells were ~80% confluent, MET at concentrations of 0.1, 0.5, 1 and 2 mM at room temperature was added to the culture medium for 24 h (19). Subsequently, 10 μl Cell Counting Kit (CCK)-8 was added into each well. The culture plates were put into the 37˚C incubator for 30 min to 4 h and OD value was measured at 450 nm with a microplate reader. The cell survival rate was calculated using a CCK (Dojindo Molecular Technologies, Inc.) in accordance with the manufacturer's instructions. Cell survival rate=[(As-Ab)/(Ac-Ab)] x100% (where As=the OD value of culture medium contained cells treated with different concentrations of metformin and CCK-8; Ac=the OD value of culture medium contained cells treated without metformin but with CCK-8; and Ab=the OD value of culture medium contained without cells but with CCK-8).

Transfection efficiency. To determine the transfection efficiency of the three different siRNAs, AML12 cells were cultured in 12-well plates and divided into control (the cells without siRNA), siRNA1, siRNA2 and siRNA3 groups. The three different siRNA transfection complexes at a concentration of 50 nM were added to the medium. Transfection efficiency of the different siRNAs was tested by reverse transcription-quantitative PCR after transfection for 24 h to determine the optimal siRNA for use in subsequent experiments.

Transfection and treatment. The AML12 cells were seeded into six-well plates when reached ~40% confluency at 37˚C and divided into CON, PA, PA + siRNA-NONMMUT031874.2 negative control (PA + siRNA-NC), PA + siRNA-NONMMUT031874.2 knockdown (PA + siRNA-NONMMUT031874.2) and PA + MET 1 mM groups (PA + MET). Transfection was performed when cells reached ~60% confluency. A total of 24 h after transfection, PA and MET were added to the corresponding groups for an additional 24 h at 37˚C before glucose concentration was measured using the glucose oxidase assay kit. RNA was also extracted for RT-qPCR and the cells were stimulated with insulin for 40 min at 37˚C in order to stimulate the expression of phosphorylation indicators of the insulin signaling pathway. Protein was extracted for western blot analysis.

Western blotting. Total protein was extracted from the liver tissues using RIPA buffer (Wuhan Servicebio Technology Co., Ltd.) and the protein concentration was determined using a BCA kit (Thermo Fisher Scientific, Inc.) Different concentrations of SDS-PAGE separation gel (8,10 and 12%) were prepared according to different molecular weights of the target proteins. After electrophoresis, proteins (amount of liver tissue protein loaded per lane was 40 μg; amount of cell protein loaded per lane was 30 μg) were transferred onto PVDF membranes. The membranes were blocked with 5% skimmed milk at room temperature for 2 h and incubated with primary antibodies overnight at 4˚C. The membranes were then washed three times with Tris-buffered saline Tween-20 (20%) solution and incubated with secondary antibodies [HRP-labeled goat anti-rabbit IgG antibody (1:8,000; cat. no. L3012-2) or goat anti-mouse IgG antibody (1:3,000; cat. no. L3032-2), all purchased from Signalway Antibody LLC] at room temperature for ~50 min. The membranes were washed and immersed in chemiluminescence solution (cat. no. G2014; Beijing Solarbio Science & Technology Co., Ltd.) for about 2 min before images were acquired. Image J software 1.8.0 (National Institutes of Health) was used to calculate the grayscale value of the developed images. The primary antibodies used were diluted as follows: β-actin (mouse antibody; 1:1,000; cat. no. 3700S); AKT (rabbit antibody; 1:2,000; cat. no. 9272S); phosphorylated (p-)AKT (Ser473) (rabbit antibody; 1:1,000; cat. no. 4060S); PI3K (rabbit antibody; 1:1,000; cat. no. 4249S); p-PI3K (rabbit antibody, 1:2,000; cat. no. 4228S); phosphoenolpyruvate carboxykinase (PEPCK; rabbit antibody; 1:2,000; cat. no. 6924S) and suppressor of cytokine signaling 3 (SOCS3; rabbit antibody; 1:1,000; cat. no. 52113S). All primary antibodies were purchased from Cell Signaling Technology, Inc.

Total RNA, miRNA and lncRNA extraction and RT-qPCR. Total RNA was extracted from the mouse liver tissues (from CON group, HFD group and HFD + MET group) using the RNAsimple Total RNA Kit (Tiangen Biotech Co., Ltd.), before RNA concentration was determined using the NanoDrop® 2000 (Thermo Fisher Scientific, Inc.). RNA was reverse transcribed into cDNA using a PrimeScript™ RT reagent kit with gDNA Eraser (cat. no. RR047A). Amplification was performed using a SYBR® Premix Ex Taq™ II kit (cat. no. RR820A) with an Applied Biosystems 7500 Real-Time PCR System (Thermo Fisher Scientific, Inc.). The PCR conditions were: 95˚C for 10 min, followed by 40 cycles at 95˚C for 15 sec, 95˚C for 15 sec and 60˚C for 30 sec. miRNA was extracted from the mouse liver tissues (from CON group, HFD group and HFD + MET group) using the miRNA extraction and isolation kit (Tiangen Biotech Co., Ltd.). RNA concentration was determined using NanoDrop® 2000 and cDNA was generated from total RNA using a miRcute Plus miRNA First-Strand cDNA Kit from Tiangen Biotech Co., Ltd. Reactions were performed and assessed by qPCR in the Applied Biosystems 7500 Real-Time PCR System using the miRcute Plus miRNA qPCR Kit (Tiangen Biotech Co., Ltd.). The PCR conditions were: 95˚C for 15 min, followed by 40 cycles at 94˚C for 20 sec, 94˚C for 20 sec and 60˚C for 34 sec. lncRNA was extracted and RNA concentration was determined as total RNA and cDNA was generated from total RNA using a lnRcute lncRNA First-Strand cDNA Synthesis Kit (With gDNase) from Tiangen Biotech Co., Ltd. Reactions were performed and assessed by qPCR in the Applied Biosystems 7500 Real-Time PCR System using the lnRcute lncRNA qPCR kit (Tiangen Biotech Co., Ltd.). The PCR conditions were: 95˚C for 3 min, followed by 40 cycles at 95˚C for 5 sec, 60˚C for 10 sec and 72˚C for 15 sec. Target gene expression levels were normalized to those of β-actin mRNA using the $2^{-\Delta\Delta Cq}$ method (20). The sequences of the primers used for qPCR in the present study are listed in Table I.

High-throughput sequencing. To obtain the hepatic gene expression profile after metformin treatment, four mice were randomly selected from each group for high-throughput sequencing. Total RNA from liver tissue was extracted in

Table I. Reverse transcription-quantitative PCR primers used in the present study.

Gene	Forward primer (5'-3')	Reverse primer (5'-3')
β-actin	GTGACGTTGACATCCGTAAAGA	GTAACAGTCCGCCTAGAAGCAC
NONMMUT031874.2	ATTTGCGTGGGACTTATCTTCAG	GAGTTAGGCTGGGTGAAGGAGA
NONMMUT149180.1	TTTATGGGCTGAAACAGGTGC	GGGCAAGAAGTCACCTGGAGT
NONMMUT153838.1	CGTGTAAATGCCTGTTGAGTGG	ATAGGGACTGAACACCTGATGCC
NONMMUT119418.1	CATTCTAAGGCTGTCTAAGGGTGA	CTCAGGTTAGCAGGAGGTTGG
NONMMUT051032.2	CAGAATGGTAATGTGGACAGGAAG	AGGATAGGGATGGTGGCAAAGT
NONMMUT153848.1	TGATGAAAGAGGTCAACGGGAT	TCATAACAGGTCCCTTGGCAGT
NONMMUT026710.2	CCCAGTAATCACTCAGGCACAA	CGTTTATCTTTCTCCTGTTCCCTC
microRNA-7054-5p	ACACTCCAGCTGGGTAGG AAGGTGGTTGGGCTG	CTCAACTGGTGTCGTGGAGTCG GCAATTCAGTTGAGAGTACTCA
U6	CTCGCTTCGGCAGCACA	AACGCTTCACGAATTTGCGT
AKT	AAGGAGGTCATCGTCGCCAA	ACAGCCCGAAGTCCGTTATC
PI3K	AAACTCCGAGACACTGCTGATG	GCTGGTATTTGGACACTGGGTAG
Glucose-6-phosphatase catalytic-subunit	ATCTTGTGGTTGGGATTCTGGG	CTGACAAGACTCCAGCCACGAC
Suppressor of cytokine signaling 3	CGCCCCCAGAATAGATGTAGTA	GACCAAGAACCTACGCATCCA
Phosphoenolpyruvate carboxykinase	GTGTTTACTGGGAAGGCATCG	ACACCTTCAGGTCTACGGCCA

accordance with the RNeasy Mini kit protocol (Qiagen GmbH). The extracted total RNA was quality inspected using the Agilent Bioanalyzer 2100 (Agilent Technologies, Inc.) and quantified using a Qubit® 3.0 Fluorometer and NanoDrop® One spectrophotometer. TruSeq™ RNA Sample Preparation Kit (Illumina, Inc.) was used to construct a sequencing library. In accordance with the instructions of Illumina NovaSeq 6000 (Illumina, Inc.), reagents for sequencing (NovaSeq 5000/6000, S4 300 Cycle; cat. no. 20012866; Illumina, Inc.) were prepared. Paired-end sequencing was performed (lncRNA ≥200 nt). Clusters were generated by cBot after the library was diluted to 10 pM and then were sequenced on the Illumina NovaSeq 6000 platform (Illumina, Inc.). The fragments of each gene segment were counted after comparison using the Stringtie software (version: 1.3.0; Johns Hopkins University, Baltimore, MD, USA) and normalized by using TMM (trimmed mean of M values) algorithm (http://www.kegg.jp/), before the fragments per kilobase million (FPKM) value of each gene was calculated. High-throughput sequencing results were uploaded onto the GEO database under the accession number GSE137840.

Analysis of differential lncRNA and mRNA expression. Differentially-expressed genes in each group were determined using the edge package for R (21) (version R-3.4.3) based on the FPKM value. The threshold values of the P-values were then adjusted by controlling for the false discovery rate. LncRNAs and mRNAs were considered to be differentially expressed at $P<0.05$ and the absolute value of Log2(fold-change) was >1.

Functional group analysis. The Gene Ontology (GO) (22) and the Kyoto Encyclopedia of Genes and Genomes (KEGG) (23) pathways determined the potential role of the lncRNAs that were co-expressed with the differentially expressed mRNAs. The GO analysis was conducted to establish significant annotations of genes and gene products in diversified organisms using the DAVID database (http://david.abcc.ncifcrf.gov). In addition, the KEGG pathway analysis was used to identify differentially expressed mRNAs in enriched pathways. After the calculated P-value was corrected by multiple hypothesis testing, a Q-value ≤0.05 was used as the threshold. Meeting this condition was defined as the GO and KEGG results that were significantly enriched for differentially expressed genes.

Clustering heat map. Heatmap was plotted by http://www.bioinformatics.com.cn, a free online platform for data analysis and visualization.

Venn diagrams. Venny (2.1.0; https://bioinfogp.cnb.csic.es/tools/venny/index.html) was used to make the Venn diagrams.

Construction of LncRNA-miRNA-mRNA co-expression network. The present study used Cytoscape (version 3.8.2) is a network visualization software with multiple applications for network analysis. It can be downloaded for free from http://www.cytoscape.org/.

Statistical analysis. SPSS v26.0 software (IBM Corp.) was used for statistical analyzes. The results were expressed as the mean ± standard deviation. An independent samples t-test (Student's t-test) was used for two-sample comparisons and one-way analysis of variance (ANOVA) followed by Bonferroni's multiple comparison test or Tamhane's multiple comparison test for multiple-sample analysis if the data

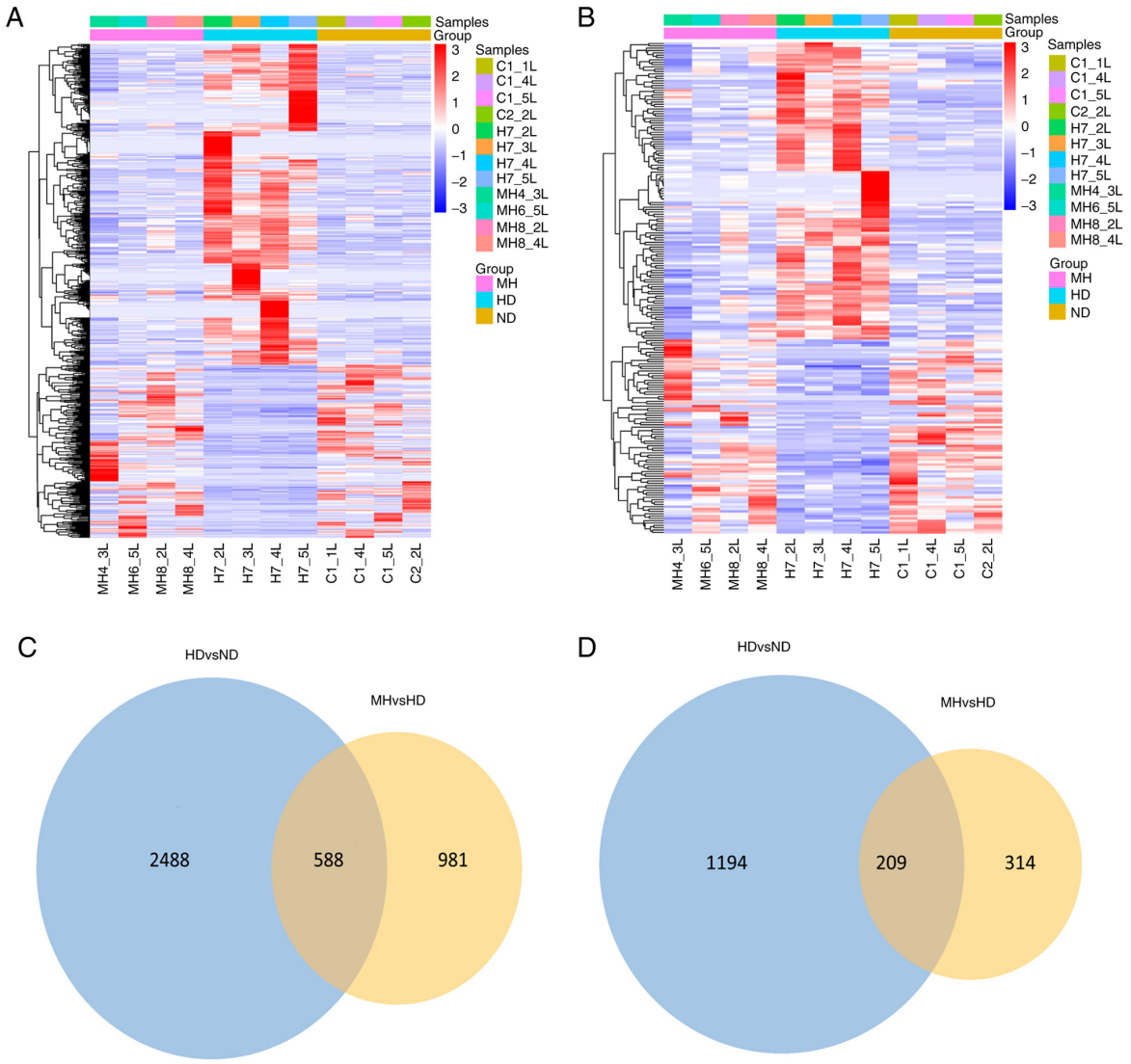

Figure 1. Differentially expressed lncRNAs and mRNAs analysis. Clustering heat map of differentially expressed (A) lncRNAs and (B) mRNAs (red area contains upregulated lncRNAs or mRNAs; blue area contains downregulated lncRNAs or mRNAs). Venn diagrams of differentially expressed (C) lncRNAs and (D) mRNAs. HD, high-fat diet; ND, normal diet; MH, high-fat diet with metformin treatment.

was normally distributed. One-Sample K-S Test to test the normality of this data. Differences were considered to be statistically significant at $P<0.05$.

Results

Differential expression of lncRNAs and mRNAs. The expression levels of lncRNAs and mRNAs in the livers of mice were determined using high-throughput sequencing and comparisons were made between the groups. Compared with the CON group, the HFD group had 3,076 differentially-expressed lncRNAs (1,823 upregulated and 1,253 downregulated) and 1,403 differentially-expressed mRNAs (892 upregulated and 511 downregulated). Compared with the HFD group, the HFD + MET group had 1,569 differentially-expressed lncRNAs (702 upregulated and 867 downregulated) and 523 differentially-expressed mRNAs (216 upregulated and 307 downregulated). Clustering heat map (Fig. 1A and B) was used to reveal the trend distribution of lncRNAs and mRNAs with a differential expression [red area contains upregulated lncRNA or mRNA with $P<0.05$ and Log2(fold-change)>1; blue area contains downregulated lncRNA or mRNA with $P<0.05$ and Log2(fold-change)<-1]. Among the 3,076 differentially-expressed lncRNAs and 1,403 differentially-expressed mRNAs in the HFD group compared with the CON group, there were 588 lncRNAs and 209 mRNAs reversed by MET (Fig. 1C and D). Moreover, among the upregulated lncRNAs and mRNAs in the HFD group compared with those in the CON group, 386 lncRNAs and 127 mRNAs were downregulated in the HFD + MET group. Among the lncRNAs and mRNAs found to be downregulated in the HFD group compared with those in the CON group, 202 lncRNAs and 82 mRNAs were upregulated in the HFD + MET group (Tables SI and SII). The top 30 differentially expressed lncRNAs and mRNAs are listed in Tables II and III.

GO and KEGG analysis. To investigate the biological functions and pathways of the differentially-expressed genes, GO

Table II. Top 30 differentially-expressed lncRNAs found in mice fed with ND, HD or MH.[a]

A, HD vs. ND

LncRNA_ID	Log_2FC	P-value	Up- or downregulated
NONMMUT149179.1	4.587344	$4.11x10^{-16}$	Up
NONMMUT031874.2	4.412077	$3.40x10^{-15}$	Up
NONMMUT153837.1	3.509002	$6.13x10^{-15}$	Up
NONMMUT139818.1	4.700016	$2.20x10^{-14}$	Up
NONMMUT031873.2	4.846336	$8.05x10^{-14}$	Up
ENSMUST00000199788	7.080694	$1.14x10^{-13}$	Up
ENSMUST00000212322	6.351815	$1.97x10^{-12}$	Up
NONMMUT149177.1	4.814471	$2.01x10^{-11}$	Up
NONMMUT152909.1	3.385954	$2.45x10^{-10}$	Up
NONMMUT149180.1	3.426143	$3.69x10^{-10}$	Up
ENSMUST00000118437	4.989526	$6.86x10^{-10}$	Up
NONMMUT153838.1	2.507940	$9.24x10^{-10}$	Up
NONMMUT119417.1	4.483789	$1.03x10^{-9}$	Up
NONMMUT008655.2	2.726889	$5.37x10^{-9}$	Up
NONMMUT140831.1	4.278518	$8.18x10^{-9}$	Up
NONMMUT067810.2	2.177739	$1.45x10^{-8}$	Up
NONMMUT119419.1	4.715676	$2.90x10^{-8}$	Up
NONMMUT011659.2	4.924532	$3.28x10^{-8}$	Up
NONMMUT119418.1	3.196553	$3.98x10^{-8}$	Up
NONMMUT058749.2	2.983326	$1.03x10^{-7}$	Up
NONMMUT029338.2	3.507321	$1.07x10^{-7}$	Up
NONMMUT152911.1	3.175219	$1.20x10^{-7}$	Up
NONMMUT153839.1	2.507771	$1.27x10^{-7}$	Up
NONMMUT146050.1	4.117007	$1.56x10^{-7}$	Up
NONMMUT145134.1	3.648683	$2.30x10^{-7}$	Up
NONMMUT003116.2	3.639365	$2.67x10^{-7}$	Up
NONMMUT149178.1	4.336275	$3.12x10^{-7}$	Up
NONMMUT153832.1	2.498095	$4.72x10^{-7}$	Up
ENSMUST00000217474	2.698023	$5.98x10^{-7}$	Up
NONMMUT067813.2	2.012964	$7.68x10^{-7}$	Up
NONMMUT112513.1	-3.870333	$4.92x10^{-2}$	Down
NONMMUT028525.2	-2.981792	$4.84x10^{-2}$	Down
NONMMUT051032.2	-2.139169	$4.80x10^{-2}$	Down
ENSMUST00000100370	-1.840982	$4.60x10^{-2}$	Down
NONMMUT030701.2	-1.475667	$4.55x10^{-2}$	Down
NONMMUT004734.2	-3.706570	$4.54x10^{-2}$	Down
NONMMUT030717.2	-1.010771	$4.53x10^{-2}$	Down
NONMMUT143378.1	-2.187454	$4.49x10^{-2}$	Down
NONMMUT068103.2	-1.590217	$4.19x10^{-2}$	Down
NONMMUT142701.1	-2.476156	$3.96x10^{-2}$	Down
NONMMUT010586.2	-1.404184	$3.94x10^{-2}$	Down
NONMMUT054418.2	-2.816135	$3.86x10^{-2}$	Down
NONMMUT081177.1	-2.398323	$3.77x10^{-2}$	Down
NONMMUT058016.2	-1.526678	$3.73x10^{-2}$	Down
NONMMUT144899.1	-2.719617	$3.72x10^{-2}$	Down
NONMMUT149434.1	-2.230984	$3.61x10^{-2}$	Down
NONMMUT068736.2	-2.360147	$3.60x10^{-2}$	Down
NONMMUT153848.1	-1.547462	$3.50x10^{-2}$	Down
NONMMUT146925.1	-3.885423	$3.46x10^{-2}$	Down

Table II. Continued.

A, HD vs. ND

LncRNA_ID	Log_2FC	P-value	Up- or downregulated
NONMMUT153657.1	-2.718099	$3.02x10^{-2}$	Down
NONMMUT144202.1	-3.054976	$2.94x10^{-2}$	Down
NONMMUT003662.2	-2.457903	$2.84x10^{-2}$	Down
NONMMUT026710.2	-2.077911	$2.83x10^{-2}$	Down
NONMMUT115606.1	-1.594442	$2.72x10^{-2}$	Down
NONMMUT140756.1	-3.890834	$2.59x10^{-2}$	Down
NONMMUT063934.2	-1.889852	$2.58x10^{-2}$	Down
NONMMUT050116.2	-1.909026	$2.53x10^{-2}$	Down
NONMMUT153405.1	-3.774999	$2.50x10^{-2}$	Down
NONMMUT144630.1	-2.966431	$2.43x10^{-2}$	Down
NONMMUT145825.1	-4.114756	$2.36x10^{-2}$	Down

B, MH vs. HD

LncRNA_ID	Log_2FC (MH vs. HD)	P-value (MH vs. HD)	Up- or downregulated
NONMMUT149179.1	-2.251507	$2.87x10^{-6}$	Down
NONMMUT031874.2	-3.052484	$1.41x10^{-6}$	Down
NONMMUT153837.1	-2.189606	$9.70x10^{-4}$	Down
NONMMUT139818.1	-2.807093	$2.99x10^{-4}$	Down
NONMMUT031873.2	-3.461724	$4.32x10^{-5}$	Down
ENSMUST00000199788	-1.754833	$6.01x10^{-3}$	Down
ENSMUST00000212322	-6.487836	$1.43x10^{-9}$	Down
NONMMUT149177.1	-1.514689	$9.06x10^{-3}$	Down
NONMMUT152909.1	-1.698336	$1.57x10^{-4}$	Down
NONMMUT149180.1	-2.498220	$2.31x10^{-5}$	Down
ENSMUST00000118437	-1.649720	$2.96x10^{-3}$	Down
NONMMUT153838.1	-2.157470	$1.36x10^{-4}$	Down
NONMMUT119417.1	-1.919131	$7.18x10^{-4}$	Down
NONMMUT008655.2	-1.152254	$1.60x10^{-2}$	Down
NONMMUT140831.1	-2.064121	$3.91x10^{-4}$	Down
NONMMUT067810.2	-1.548822	$8.12x10^{-5}$	Down
NONMMUT119419.1	-1.646476	$3.06x10^{-3}$	Down
NONMMUT011659.2	-3.617385	$1.81x10^{-5}$	Down
NONMMUT119418.1	-2.804343	$5.90x10^{-6}$	Down
NONMMUT058749.2	-1.571707	$3.17x10^{-3}$	Down
NONMMUT029338.2	-1.302473	$5.84x10^{-3}$	Down
NONMMUT152911.1	-1.501832	$1.39x10^{-3}$	Down
NONMMUT153839.1	-1.853127	$1.52x10^{-3}$	Down
NONMMUT146050.1	-1.336522	$9.06x10^{-3}$	Down
NONMMUT145134.1	-2.500624	$1.43x10^{-4}$	Down
NONMMUT003116.2	-1.457044	$1.46x10^{-2}$	Down
NONMMUT149178.1	-3.414379	$3.50x10^{-5}$	Down
NONMMUT153832.1	-1.646988	$2.16x10^{-2}$	Down
ENSMUST00000217474	-1.658877	$8.94x10^{-3}$	Down
NONMMUT067813.2	-1.210335	$3.46x10^{-3}$	Down

Table II. Continued.

B, MH vs. HD

LncRNA_ID	Log_2FC (MH vs. HD)	P-value (MH vs. HD)	Up- or downregulated
NONMMUT112513.1	4.866435	$1.76x10^{-3}$	Up
NONMMUT028525.2	4.352477	$9.57x10^{-3}$	Up
NONMMUT051032.2	2.254394	$8.68x10^{-3}$	Up
ENSMUST00000100370	2.885722	$3.38x10^{-3}$	Up
NONMMUT030701.2	1.926416	$1.04x10^{-2}$	Up
NONMMUT004734.2	4.319358	$8.70x10^{-3}$	Up
NONMMUT030717.2	1.290012	$3.90x10^{-2}$	Up
NONMMUT143378.1	2.891794	$4.09x10^{-2}$	Up
NONMMUT068103.2	2.658230	$2.62x10^{-2}$	Up
NONMMUT142701.1	2.940979	$3.16x10^{-2}$	Up
NONMMUT010586.2	1.702768	$3.09x10^{-2}$	Up
NONMMUT054418.2	3.888229	$4.97x10^{-3}$	Up
NONMMUT081177.1	2.441776	$2.94x10^{-2}$	Up
NONMMUT058016.2	2.520639	$1.87x10^{-3}$	Up
NONMMUT144899.1	2.590428	$1.55x10^{-2}$	Up
NONMMUT149434.1	2.255812	$3.47x10^{-2}$	Up
NONMMUT068736.2	3.192271	$1.90x10^{-3}$	Up
NONMMUT153848.1	2.249656	$2.62x10^{-2}$	Up
NONMMUT146925.1	4.319742	$3.87x10^{-2}$	Up
NONMMUT153657.1	2.948339	$5.64x10^{-3}$	Up
NONMMUT144202.1	4.091950	$1.24x10^{-2}$	Up
NONMMUT003662.2	2.517240	$1.38x10^{-2}$	Up
NONMMUT026710.2	3.141129	$2.48x10^{-2}$	Up
NONMMUT115606.1	2.539770	$1.29x10^{-2}$	Up
NONMMUT140756.1	5.412773	$3.42x10^{-2}$	Up
NONMMUT063934.2	2.092702	$1.11x10^{-2}$	Up
NONMMUT050116.2	2.127048	$2.57x10^{-2}$	Up
NONMMUT153405.1	4.558180	$1.47x10^{-2}$	Up
NONMMUT144630.1	2.789511	$4.01x10^{-2}$	Up
NONMMUT145825.1	4.499107	$1.85x10^{-4}$	Up

[a]Top 30 of the differentially-expressed lncRNAs in the HD group compared with the ND group and those in the MH group compared with those the HD group are shown; with Fragments Per Kilobase Million=0 eliminated. The top 30 differently expressed lncRNAs (with FPKM=0 were eliminated) were ranked according ascending order of P-value (HD vs. ND). lncRNA, long non-coding RNA; ND, regular diet; HD, high-fat diet; MH, HD with metformin; FC, fold change.

enrichment and KEGG pathway analyses were performed. The top 30 enriched target genes in the GO analysis included 'response to nitrogen compound', 'positive regulation of signaling', 'chemical homeostasis', 'cellular homeostasis' and so on. Differentially-expressed mRNAs were mainly involved in the 'small cell lung cancer', 'MAPK signaling pathway', 'cellular senescence' and 'insulin signaling pathway' (Fig. 2A and B). The KEGG analysis in the GEO database indicated that the differentially-expressed mRNAs can enrich in hundreds of pathways. Although the insulin signaling pathway were enriched by a small gene number, it was also listed as a top 30 pathway. In addition, the insulin signaling pathway was statistically significant (q-values ≤0.05. Moreover, it is associated with the liver insulin resistance model of the HFD-fed mice. So the insulin signaling pathway was selected.

Establishment of an insulin-resistant mouse model induced by high-fat diet. Before HFD intervention (at baseline), there was no difference in body weight between the HFD and CON groups. After 8 weeks of high-fat diet intervention, from week 2 onwards, the weight of the mice in the HFD group was significantly higher compared with that in the CON group (Fig. 3A). There was no difference in

Table III. Top 30 differentially-expressed mRNAs found in mice fed with ND, HD or MH.[a]

A, HD vs. ND

Gene name	Log_2FC (HD vs. ND)	P-value (HD vs. ND)	Up- or downregulated
Cfd	7.102398	$1.24x10^{-50}$	Up
Aacs	3.578468	$1.97x10^{-37}$	Up
Foxq1	3.572630	$3.28x10^{-32}$	Up
Phlda1	2.502932	$5.15x10^{-30}$	Up
Chac1	3.581907	$8.30x10^{-26}$	Up
Cish	2.878978	$8.77x10^{-25}$	Up
Themis	4.129499	$1.23x10^{-20}$	Up
Gm43756	7.064607	$1.60x10^{-18}$	Up
Gm28592	3.115101	$2.17x10-^{18}$	Up
Gm28182	2.584522	$2.47x10^{-16}$	Up
3110082I17Rik	2.015142	$4.18x10-^{16}$	Up
Nrep	2.163696	$1.94x10^{-14}$	Up
Gadd45a	2.633552	$1.29x10^{-13}$	Up
Mup-ps14	4.979470	$1.24x10^{-12}$	Up
Cidea	7.449365	$2.74x10^{-12}$	Up
Aqp8	1.734631	$7.79x10^{-12}$	Up
Socs3	2.417039	$1.30x10^{-11}$	Up
Lgals1	2.525710	$1.81x10^{-11}$	Up
Mas1	5.097515	$2.27x10^{-11}$	Up
Gm26876	4.776975	$8.33x10^{-11}$	Up
Gbp11	2.976467	$1.21x10^{-10}$	Up
Adgrv1	3.122875	$1.71x10^{-10}$	Up
A530084C06Rik	2.308730	$4.86x10^{-10}$	Up
Rnf186	1.994529	$8.10x10^{-10}$	Up
Myc	2.508489	$1.58x10^{-9}$	Up
Mogat1	2.514068	$1.66x10^{-9}$	Up
Sptlc3	Inf	$1.80x10^{-9}$	Up
Gm11967	1.820830	$2.48x10^{-9}$	Up
Gm27551	5.118398	$4.13x10^{-9}$	Up
Clec2h	3.253263	$1.07x10^{-8}$	Up
Ebf3	-2.044633	$4.93x10^{-2}$	Down
Mir3068	-1.242104	$4.77x10^{-2}$	Down
Sidt1	-1.284115	$3.74x10^{-2}$	Down
Slc4a5	-2.799238	$3.66x10^{-2}$	Down
Gm45753	-3.035576	$3.57x10^{-2}$	Down
1810013D15Rik	-1.021073	$2.50x10^{-2}$	Down
Gm23445	-1.382136	$2.29x10^{-2}$	Down
Hdx	-1.163874	$2.27x10^{-2}$	Down
Mir8097	-2.901827	$2.15x10^{-2}$	Down
Gm9025	-2.463844	$2.14x10^{-2}$	Down
Gm44224	-1.537712	$1.96x10^{-2}$	Down
Adat3	-2.345512	$1.94x10^{-2}$	Down
Zfp422	-1.039810	$1.69x10^{-2}$	Down
Cabyr	-1.302456	$1.64x10^{-2}$	Down
Gm9916	-1.473988	$1.42x10^{-2}$	Down
Zfp804b	-2.264639	$1.31x10^{-2}$	Down
Psma8	-1.107980	$1.26x10^{-2}$	Down
Gm37660	-1.417403	$1.24x10^{-2}$	Down
Gm10728	-1.418026	$1.02x10^{-2}$	Down

Table III. Continued.

A, HD vs. ND

Gene name	Log_2FC (HD vs. ND)	P-value (HD vs. ND)	Up- or downregulated
Usf3	-2.087752	$8.18x10^{-3}$	Down
Gm26871	-1.281593	$6.45x10^{-3}$	Down
Rnase10	-3.779923	$5.58x10^{-3}$	Down
Snora73a	-1.659874	$3.81x10^{-3}$	Down
Gm15842	-1.072109	$3.65x10^{-3}$	Down
Ppp1r3g	-3.305166	$3.31x10^{-3}$	Down
Gm17108	-1.469128	$3.04x10^{-3}$	Down
Fkbp5	-1.052135	$3.04x10^{-3}$	Down
Abca14	-1.618418	$2.98x10^{-3}$	Down
Adgrf1	-1.341829	$2.45x10^{-3}$	Down
Gm32540	-1.422205	$2.00x10^{-3}$	Down

B, MH vs. HD

Gene name	Log_2FC (MH vs. HD)	P-value (MH vs. HD)	Up- or downregulated
Cfd	-2.051145	$1.41x10^{-6}$	Down
Aacs	-1.280914	$1.31x10^{-5}$	Down
Foxq1	-1.247545	$1.73x10^{-5}$	Down
Phlda1	-1.803304	$3.82x10^{-8}$	Down
Chac1	-1.104198	$2.48x10^{-3}$	Down
Cish	-1.621644	$6.85x10^{-3}$	Down
Themis	-1.322426	$6.50x10^{-4}$	Down
Gm43756	-1.743903	$4.41x10^{-3}$	Down
Gm28592	-2.114167	$1.51x10^{-6}$	Down
Gm28182	-2.393627	$3.18x10^{-7}$	Down
3110082I17Rik	-1.305596	$6.21x10^{-8}$	Down
Nrep	-1.336429	$5.13x10^{-9}$	Down
Gadd45a	-1.319588	$1.49x10^{-5}$	Down
Mup-ps14	-1.647291	$1.27x10^{-3}$	Down
Cidea	-2.794620	$3.40x10^{-3}$	Down
Aqp8	-1.406878	$7.08x10^{-8}$	Down
Socs3	-1.205874	$3.08x10^{-3}$	Down
Lgals1	-1.517038	$2.25x10^{-5}$	Down
Mas1	-2.845129	$1.08x10^{-5}$	Down
Gm26876	-2.916657	$9.81x10^{-5}$	Down
Gbp11	-1.385258	$2.00x10^{-4}$	Down
Adgrv1	-1.508109	$1.35x10^{-3}$	Down
A530084C06Rik	-1.067840	$3.91x10^{-3}$	Down
Rnf186	-1.238196	$1.24x10^{-5}$	Down
Myc	-2.093431	$7.47x10^{-6}$	Down
Mogat1	-1.468955	$1.19x10^{-4}$	Down
Sptlc3	-1.207829	$4.77x10^{-2}$	Down
Gm11967	-1.098758	$1.86x10^{-4}$	Down
Gm27551	-1.249623	$1.23x10^{-2}$	Down
Clec2h	-1.359496	$3.48x10^{-3}$	Down
Ebf3	2.890585	$9.42x10^{-3}$	Up
Mir3068	1.482346	$4.88x10^{-2}$	Up

Table III. Continued.

B, MH vs. HD

Gene name	Log_2FC (MH vs. HD)	P-value (MH vs. HD)	Up- or downregulated
Sidt1	1.676417	$1.47x10^{-2}$	Up
Slc4a5	3.203330	$1.43x10^{-2}$	Up
Gm45753	4.141122	$1.21x10^{-6}$	Up
1810013D15Rik	1.251620	$3.89x10^{-2}$	Up
Gm23445	1.588164	$2.10x10^{-2}$	Up
Hdx	1.344117	$1.83x10^{-2}$	Up
Mir8097	3.678148	$6.22x10^{-3}$	Up
Gm9025	3.684024	$4.36x10^{-3}$	Up
Gm44224	1.637062	$1.01x10^{-2}$	Up
Adat3	2.330407	$1.92x10^{-2}$	Up
Zfp422	1.049609	$2.75x10^{-2}$	Up
Cabyr	1.323208	$1.51x10^{-4}$	Up
Gm9916	1.350597	$2.45x10^{-2}$	Up
Zfp804b	2.430546	$3.73x10^{-2}$	Up
Psma8	1.499127	$3.45x10^{-4}$	Up
Gm37660	1.756026	$1.43x10^{-2}$	Up
Gm10728	2.111559	$6.16x10^{-3}$	Up
Usf3	2.199649	$6.10x10^{-5}$	Up
Gm26871	1.201270	$6.46x10^{-3}$	Up
Rnase10	3.843550	$8.34x10^{-3}$	Up
Snora73a	1.662650	$2.33x10^{-2}$	Up
Gm15842	1.222220	$7.11x10^{-3}$	Up
Ppp1r3g	2.804066	$1.86x10^{-4}$	Up
Gm17108	1.627575	$9.72x10^{-3}$	Up
Fkbp5	1.373474	$3.92x10^{-3}$	Up
Abca14	1.280070	$3.85x10^{-2}$	Up
Adgrf1	1.164962	$1.51x10^{-2}$	Up
Gm32540	1.100892	$4.52x10^{-2}$	Up

[a]Top 30 of the differentially-expressed mRNAs in the HD group compared with the ND group and those in the MH group compared with those the HD group were shown; with Fragments Per Kilobase Million=0 were eliminated. ND, regular diet; HD, high-fat diet; MH, HD with metformin; FC, fold change.

the average daily caloric intake between the two groups (Fig. 3B).

IPGTT experiment was performed after feeding on a HFD for 8 weeks. Compared with that in the CON group, the blood glucose levels in the HFD group were significantly increased at 0, 30, 60 and 120 min (Fig. 3C). However, there was no difference at 15 min (Fig. 3C). Compared with that in the CON group, the AUC in the HFD group was significantly increased (Fig. 3D), suggesting that the insulin-resistant mouse model had been successfully established.

Changes in body weight and insulin resistance of mice in each group after MET intervention for 6 weeks. The body weight in the HFD group was significantly higher compared with that in the CON group for 8 weeks. After MET intervention for 3 weeks onwards, the body weight of mice in the HFD + MET group was significantly decreased compared with that in the HFD group (Fig. 3E). There was no difference in the daily food intake among the three groups (Fig. 3F).

IPGTT results after MET intervention for 6 weeks. IPGTT assay was performed after MET intervention for 6 weeks. Compared with that in the CON group, blood glucose levels in the HFD group were significantly higher at 0, 30, 60 and 120 min (Fig. 3G). In addition, blood glucose levels in the HFD + MET group were significantly lower compared with those in the HFD group (Fig. 3G). There was no difference in blood glucose levels among the three groups at 15 min (Fig. 3G). The AUC in the HFD group was significantly higher compared with that in the CON group, but was significantly

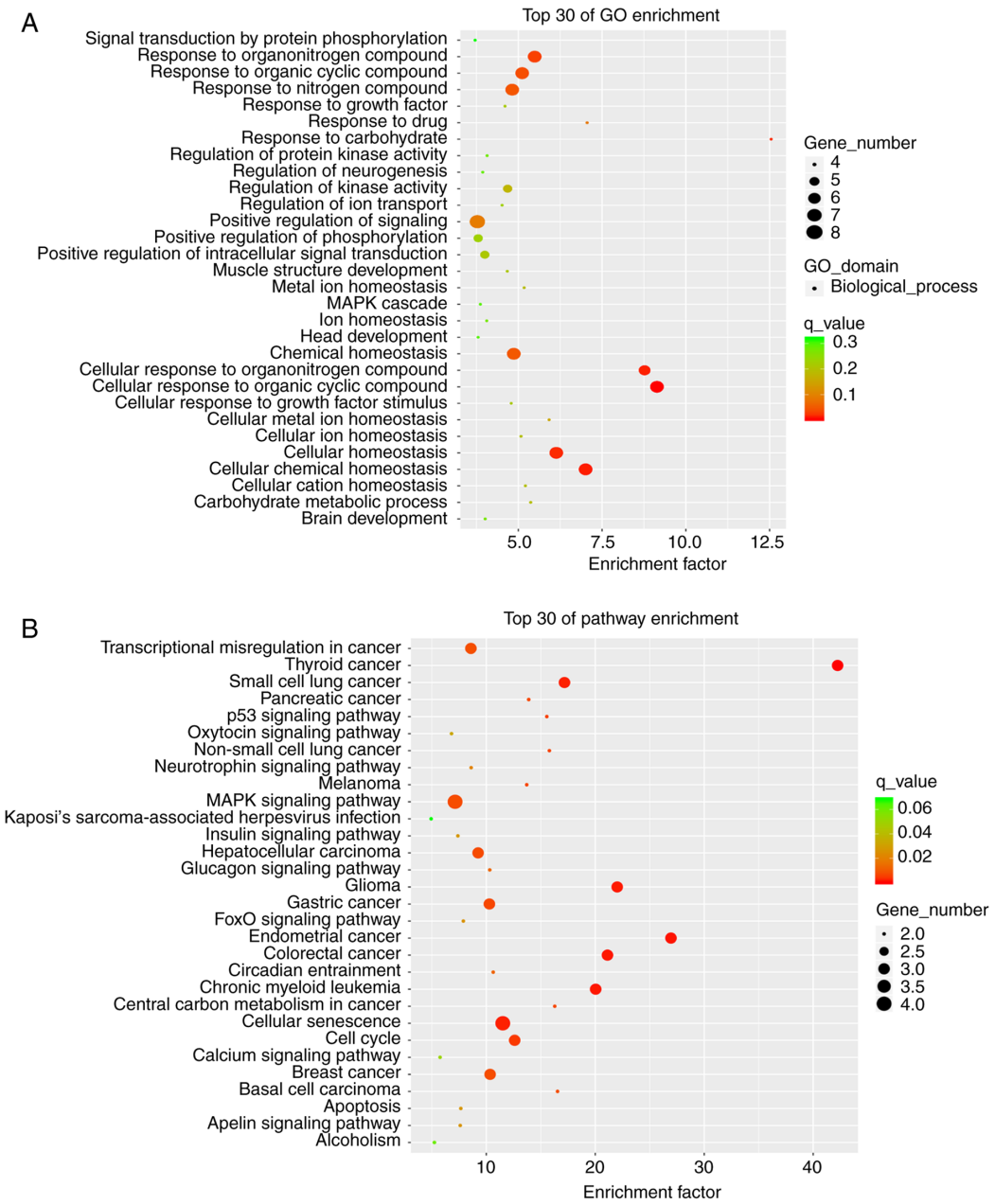

Figure 2. GO and KEGG analysis. (A) Top 30 GO terms of the differentially expressed mRNAs. (B) Top 30 pathways with significant functional changes of the differentially expressed mRNAs. The X-axis of (A) and (B) were 'Enrichment factor', lncRNA, long non-coding RNA; GO, gene ontology; KEGG, Kyoto Encyclopaedia of Genes and Genomes.

lower in the HFD + MET group compared with that in the HFD group (Fig. 3H).

Blood glucose, insulin and QUICKI of mice in the three groups. Compared with those in the CON group, the fasting blood glucose and insulin levels in the HFD group were significantly increased, whilst the QUICKI value was significantly decreased (Fig. 3I-K). Compared with those in the HFD group, the fasting blood glucose and insulin levels in the HFD + MET group were significantly decreased, but the QUICKI value was increased significantly (Fig. 3I-K). These results suggest that MET can improve insulin sensitivity in insulin-resistant mice.

Blood lipid levels in the three groups. Compared with those in the CON group, the levels of TC, TG, LDL-C and FFA in the HFD group were significantly higher, whilst those of HDL-C were significantly lower (Fig. 4A-E). Compared with those in the HFD group, the levels of TC, TG and FFA in the HFD + MET group were significantly decreased whereas the levels of HDL-C were significantly increased. There was no change in the levels of LDL-C between the HFD and HFD + MET groups (Fig. 4A-E).

Expression of mRNAs and proteins related to the insulin signaling pathway. RT-qPCR results showed that compared with those in the CON group, the mRNA expression levels of SOCS3, PEPCK and glucose-6-phosphatase catalytic subunit (G6PC) in the liver tissues of the HFD group mice were significantly increased, which were significantly reversed by MET treatment (Fig. 4H-J). However, the mRNA expression

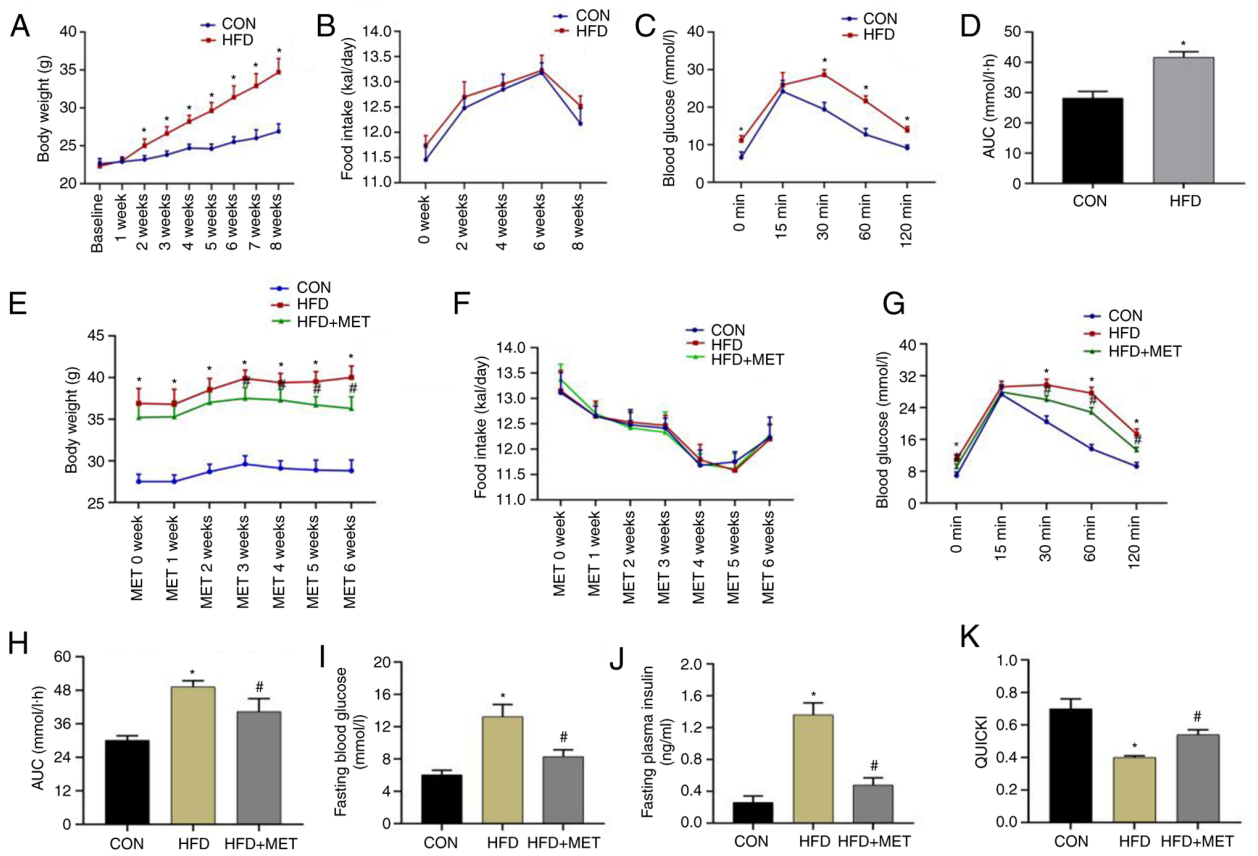

Figure 3. Establishment of the insulin resistance model in mice and changes in insulin resistance after MET intervention for 6 weeks. (A-D) Body weight, food intake, IPGTT and AUC results of mice before and after feeding on a HFD for 8 weeks. (A) Body weight. (B) Food intake. (C) Blood glucose levels were measured at 0, 15, 30, 60 and 120 min after intraperitoneal glucose injection. (D) AUC of blood glucose from Fig. 2C. Data are presented as the mean ± SD (CON n=14; HFD n=28). *P<0.05 vs. CON. (E-H) Body weight, food intake, IPGTT and AUC results of mice after MET treatment for 6 weeks. (E) Body weight. (F) Food intake. (G) Blood glucose levels were measured at 0, 15, 30, 60 and 120 min after intraperitoneal glucose injection. (H) AUC of blood glucose from Fig. 2G. Data are presented as the mean ± SD (n=14). *P<0.05 vs. CON and #P<0.05 vs. HFD. (I-K) Fasting blood glucose, fasting plasma insulin and QUICKI after MET treatment for 6 weeks. (I) Fasting blood glucose levels. (J) Fasting plasma insulin levels. (K) QUICKI calculations. Data are presented as the mean ± SD (n=10). *P<0.05 vs. CON and #P<0.05 vs. HFD. IPGTT, intraperitoneal glucose tolerance test; HFD, high-fat diet; QUICKI, quantitative insulin sensitivity check index; AUC, area under the curve; MET, metformin.

levels of PI3K and AKT had no significant difference in the three groups (Fig. 4F and G). Western blot analysis showed that compared with those in the CON group, the expression levels of SOCS3 and PEPCK were significantly increased in the HFD group, which were significantly reversed by MET treatment (Fig. 5). Analysis of PI3K and AKT phosphorylation revealed that they were significantly reduced in the HFD group compared with those in the CON group (Fig. 5). By contrast, PI3K and AKT phosphorylation in the HFD + MET group was significantly higher compared with that in the HFD group (Fig. 5).

Verification of the differentially-expressed lncRNAs in the liver of mice. Among the lncRNAs found to be differentially expressed after MET treatment in mice in the HFD group, three lncRNAs that were upregulated by HFD and subsequently downregulated by MET treatment (NONMMUT153838.1, NONMMUT031874.2 and NONMMUT119418.1) and two lncRNAs showing the opposite pattern (NONMMUT051032.2 and NONMMUT153848.1) were randomly selected to be analyzed. RT-qPCR analysis verified that the expression pattern of these five lncRNAs was consistent with the results of high-throughput sequencing analysis (Fig. 6A-E).

LncRNA-miRNA-mRNA co-expression network. Among the verified lncRNAs, NONMMUT031874.2 was highly expressed compared with the other verified lncRNAs. The KEGG analysis indicated that SOCS3 played a notable role in the insulin signaling pathway. In the latter, SOCS3 was reportedly involved in the development of IR (24). To assess this potential interaction, a lncRNA-miRNA-mRNA-related network was constructed and the results showed that NONMMUT031874.2 may regulate SOCS3 expression by interacting with miR-7054-5p, miR-7669-3p, miR-1894-3p, miR-7016-3p and miR-7076-5p (Fig. 7A).

LncRNA-miRNA-mRNA base-pairing diagram. To explore the potential molecular mechanism of NONMMUT031874.2, NONCODE (http://www.noncode.org/) and miRBase online databases (http://www.mirbase.org/index.shtml) were used, which showed that the mouse NONMMUT031874.2 sequence contains an miR-7054-5p binding site. In addition, the Targetscan database (http://www.targetscan.org/vert_71/) also predicted that SOCS3 is a target gene of miR-7054-5p (Fig. 7B and C). These results suggest that NONMMUT031874.2 may regulate the expression of SOCS3 through miR-7054-5p.

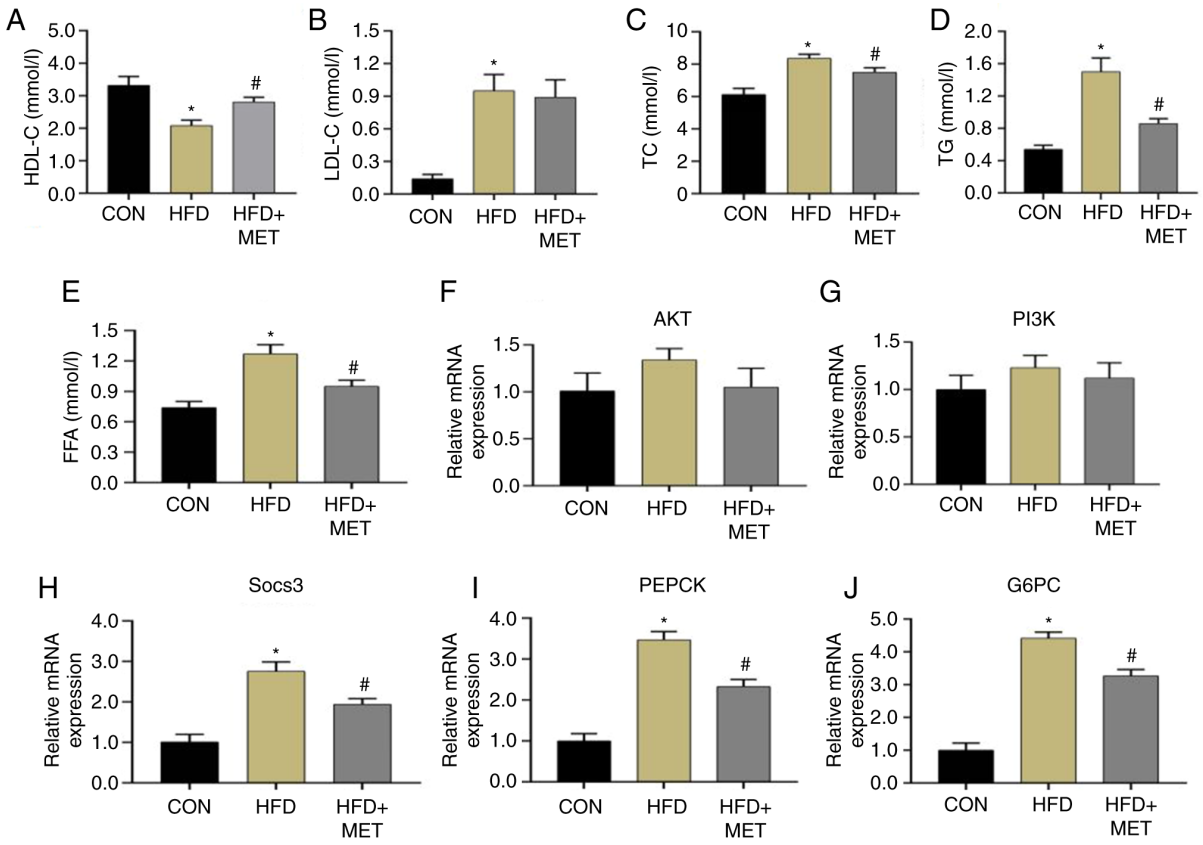

Figure 4. Blood lipid levels and mRNA expression of components in the insulin signaling pathway in mice from different groups. (A-E) Blood lipid parameters were measured after MET intervention. (A) HDL-C, (B) LDL-C, (C) TC, (D) TG and (E) FFA. Data are presented as the mean ± SD (n=10). *P<0.05 vs. CON and #P<0.05 vs. HFD. (F-J) Relative mRNA expression of components in the insulin signaling pathway in liver tissues. (F) AKT, (G) PI3K, (H) Socs3, (I) PEPCK and (J) G6PC. Data are presented as the mean ± SD (n=6). *P<0.05 vs. CON and #P<0.05 vs. HFD. CON, control; HFD, high-fat diet; MET, metformin; HDL-C, high-density-lipoprotein cholesterol; LDL-C, low-density-lipoprotein cholesterol; TC, total cholesterol; TG, triglyceride; FFA, free fatty acid; Socs3, suppressor of cytokine signaling 3; PEPCK, phosphoenolpyruvate carboxykinase; G6PC, glucose-6-phosphatase catalytic-subunit.

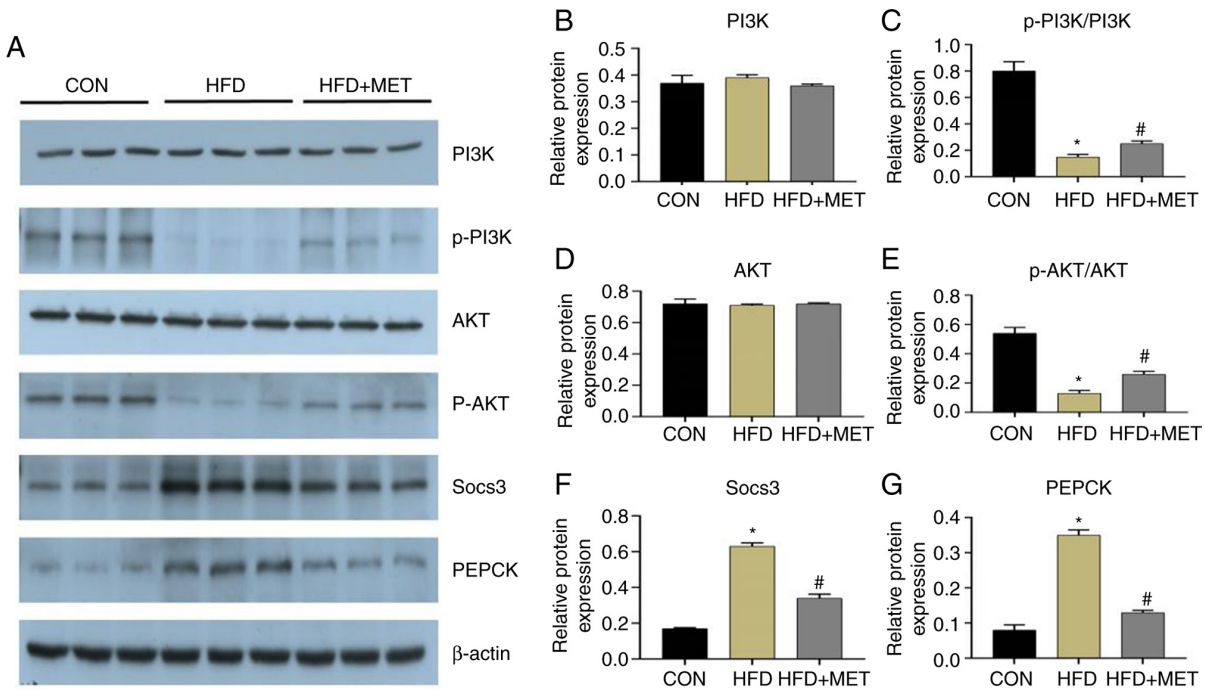

Figure 5. Expression of proteins related to the insulin signaling pathway in mice in different groups. (A) Representative western blotting images of proteins in the insulin signaling pathway. (B) PI3K; (C) p-PI3K/PI3K; (D) AKT; (E) p-AKT/AKT; (F) Socs3; (G) PEPCK. Data are presented as the mean ± SD (n=3). *P<0.05 vs. CON and #P<0.05 vs. HFD. CON, control; HFD, high-fat diet; MET, metformin; p-, phosphorylated; SOCS3, suppressor of cytokine signaling 3; PEPCK, phosphoenolpyruvate carboxykinase.

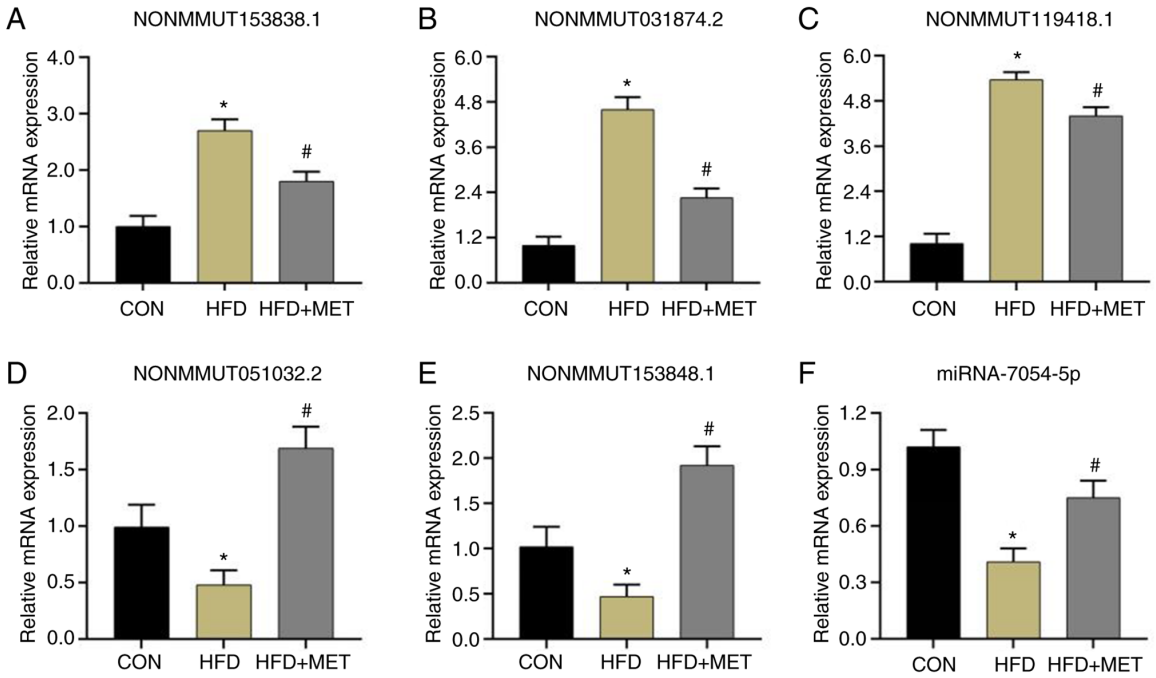

Figure 6. Verification of the differentially-expressed lncRNAs and miRNA in the liver tissues of mice. (A-C) Verification of HFD-upregulated and MET-downregulated lncRNAs by RT-qPCR. (A) NONMMUT153838.1, (B) NONMMUT031874.2 and (C) NONMMUT119418.1. Verification of the HFD-downregulated and MET-upregulated lncRNAs by RT-qPCR. (D) NONMMUT051032.2 (E) NONMMUT153848.1 and (F) miR-7054-5p. Data are presented as the mean ± SD (n=6). *P<0.05 vs. CON and #P<0.05 vs. HFD. CON, control; HFD, high-fat diet; MET, metformin; LncRNA, long non-coding RNA; miRNA, microRNA; RT-qPCR, reverse transcription-quantitative PCR.

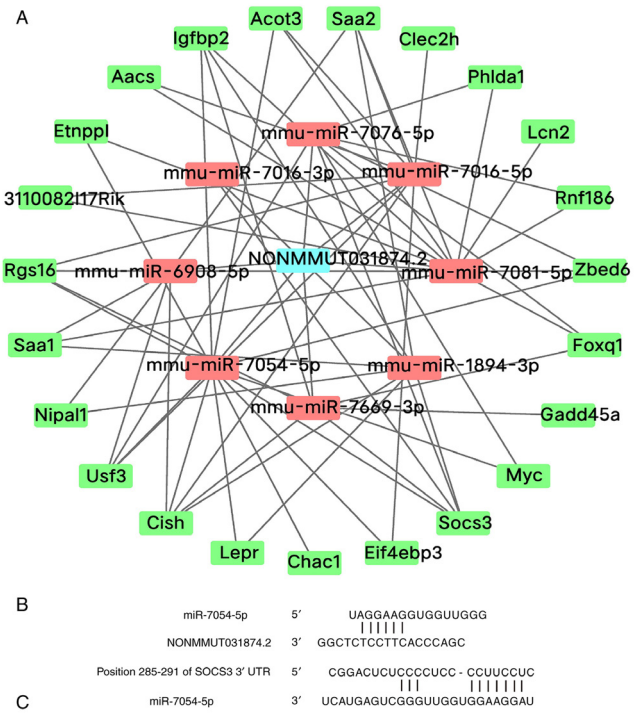

Figure 7. Network and target gene analysis. (A) LncRNA NONMMUT031874.2-miRNA-mRNA co-expression network. (B) Positions of miR-7054-5p binding sites on NONMMUT031874.2 are shown. (C) Positions of the miR-7054-5p binding sites on SOCS3 are shown. SOCS3, suppressor of cytokine signaling 3; lncRNA, long non-coding RNA; miR, microRNA; UTR, untranslated region.

miRNA-7054-5p expression in liver tissues of mice in the three groups. The expression of miR-7054-5p in the liver tissues was measured by RT-qPCR. The expression of miR-7054-5p mRNA in the HFD group was significantly decreased compared with that in the CON group, whilst its expression was significantly increased in the HFD + MET group compared with that in the HFD group (Fig. 6F).

Establishment of an in vitro model of insulin resistance. The insulin resistance model was established in AML12 cells by treatment with PA, before the glucose concentrations in the culture medium at 0, 8, 16 and 24 h after PA intervention were measured. At 0 and 8 h, the glucose concentration in the medium showed no significant difference between the CON and PA groups. By contrast, at 16 and 24 h, the glucose concentration in the PA group was higher compared with that in the CON group, suggesting that the *in vitro* insulin resistance model had been successfully established (Fig. 8A). This could be seen as after 24 h of treatment with PA in AML12 cells, the glucose concentration in the culture medium of the PA group was significantly higher compared with that of the Con group, which indicated that the gluconeogenesis of these cells was significantly increased due to the PA, and more glucose was released into the culture medium. Therefore, it can be demonstrated that the insulin resistance model was successfully established.

Cell viability assay. AML12 cells were treated with different concentrations of MET (0.1, 0.5, 1 and 2 mM). MET at a concentration of 2 mM significantly reduced cell viability compared with that in the CON group (Fig. 8B). To observe the effect of MET on cells after PA intervention, 1 mM was selected as the MET concentration for further functional analysis. The cell survival rate did not differ significantly among the three groups (Fig. 8C).

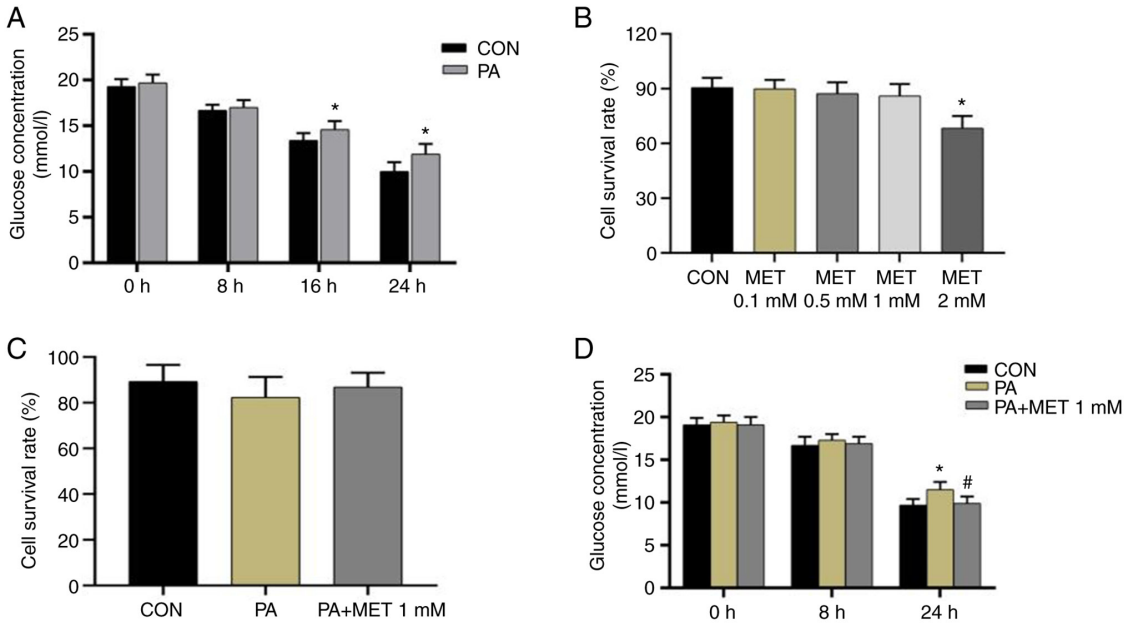

Figure 8. Establishment of an *in vitro* model of insulin resistance and changes in glucose concentration after PA and MET treatment. (A) Glucose concentration in the culture medium after PA treatment for 0, 8, 16 and 24 h. Data are presented as the mean ± SD (n=6). *P<0.05 vs. CON. (B) Cell survival rates after treatment with different concentrations of MET for 24 h. (C) Cell survival rates of cells in the different groups after PA and MET treatments. (D) Glucose concentrations in the culture medium after PA and MET treatment for 0, 8 and 24 h. Data are presented as the mean ± SD (n=6). *P<0.05 vs. CON and $^{\#}$P<0.05 vs. PA. CON, control; PA, palmitic acid; MET, metformin.

Changes in glucose concentration after PA and MET treatment. After the cells were treated with PA and 1 mM MET, no significant difference in glucose concentration could be found among the three groups at 0 and 8 h. However, compared with those in the CON group, the media glucose levels in the PA group were significantly increased at 24 h. After treatment with MET, the glucose levels were significantly decreased at 24 h (Fig. 8D).

Verification of lncRNAs in AML12 cells. Among the lncRNAs that were differentially expressed by MET treatment after HFD feeding and then verified, two lncRNAs that were upregulated by HFD and reversed by MET (NONMMUT031874.2 and NONMMUT149180.1) and two lncRNAs that exhibited the opposite pattern (NONMMUT153848.1 and NONMMUT026710.2) were randomly selected. The AML12 cell RNA samples were subjected to RT-qPCR to verify the sequencing results in AML12 cells. As shown by RT-qPCR, it was shown that the expression patterns of these four lncRNAs were consistent with the results of sequencing analyses of the mouse liver samples (Fig. 9A-D).

Expression of NONMMUT031874.2 mRNA after different siRNAs were transfected into AML12 cells. After the three different siRNAs were transfected into AML12 cells for 24 h, the results of RT-qPCR showed that, compared with those in the CON group (the cells without siRNA), the expression levels of NONMMUT031874.2 in the three siRNA groups were significantly decreased. Compared with the levels in the siRNA1 and siRNA2 groups, NONMMUT031874.2 expression in the siRNA3 group was lower, with the difference significant compared with siRNA2. This suggested that the knockdown efficiency of siRNA3 was the most efficient, which was used for subsequent experiments (Fig. 9E).

Expression of NONMMUT031874.2 mRNA in the CON, PA, PA + siRNA-NC, PA + siRNA-NONMMUT031874.2 and PA + MET groups. After NONMMUT031874.2 siRNA transfection into AML12 cells, compared with that in the CON group, the expression of NONMMUT031874.2 in the PA and the PA + siRNA-NC groups was significantly increased. In addition, the expression of NONMMUT031874.2 in the PA + siRNA-NONMMUT031874.2 and PA + MET groups was significantly decreased compared with that in the PA group. There was no difference between the PA + siRNA-NONMMUT031874.2 group and the PA + MET group (Fig. 9F).

Expression of miR-7054-5p mRNA after knocking down NONMMUT031874.2 expression. After siRNA transfection into AML12 cells, compared with that in the CON group, the expression of miR-7054-5p was significantly decreased in the PA and PA + siRNA-NC groups. In addition, the expression of miR-7054-5p in the PA + siRNA-NONMMUT 031874.2 and PA + MET groups was significantly increased compared with that in the PA group. The expression levels in the PA + siRNA-NONMMUT031874.2 and PA + MET groups did not differ from each other (Fig. 9G).

Changes in glucose concentration after NONMMUT031874.2 knockdown. After siRNA transfection into AML12 cells, the glucose concentration in the medium of cells in the PA and PA + siRNA-NC groups were significantly increased compared with that in the CON group. Additionally, the glucose concentration of cells in the PA + siRNA-NONMMUT031874.2 and PA + MET groups were significantly decreased compared

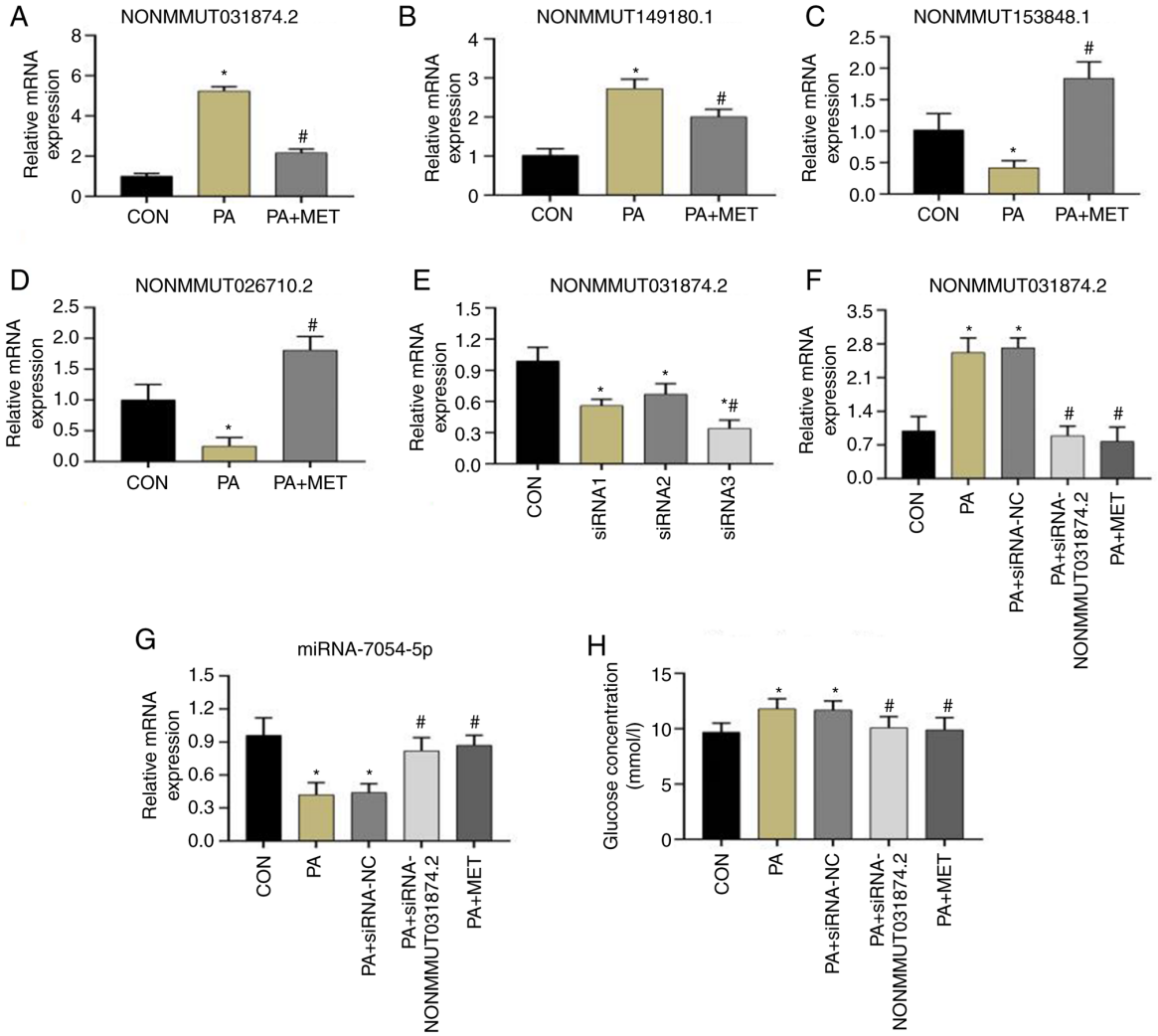

Figure 9. Verification of the differentially-expressed lncRNAs and miRNA in AML12 cells and changes in glucose concentration after NONMMUT031874.2 knockdown or MET in different groups. (A-D) Verification of the differentially-expressed lncRNAs by reverse transcription-quantitative PCR. (A) NONMMUT031874.2, (B) NONMMUT149180.1, (C) NONMMUT 153848.1 and (D) NONMMUT026710.2. Data are presented as the mean ± SD (n=6). *P<0.05 vs. CON and #P<0.05 vs. PA. (E) Expression of NONMMUT031874.2 after the transfection of three different siRNAs into AML12 cells. Data are presented as the mean ± SD (n=6). *P<0.05 vs. CON and #P<0.05 vs. siRNA2. (F) Expression of NONMMUT031874.2 after siRNA transfection or MET treatment in AML12 cells in different groups. (G) Expression of miR-7054-5p after siRNA transfection or MET treatment in AML12 cells in different groups. (H) Glucose concentrations in the culture medium after siRNA transfection or MET treatment in AML12 cells in different groups. Data are presented as the mean ± SD (n=6). *P<0.05 vs. CON and #P<0.05 vs. PA. PA, palmitic acid; MET, metformin; NC, negative control; lncRNA, long non-coding RNA; miRNA or miR, microRNA; siRNA, small interfering RNA; CON, control untransfected cells.

with that in the PA group. However, there was no significant difference between the glucose levels of cells in the PA + siRNA-NONMMUT031874.2 and PA + MET groups (Fig. 9H).

Effect of MET on insulin signaling pathway after knockdown of NONMMUT031874.2. Compared with that in the CON group, the expression of SOCS3 and PEPCK in the PA and PA + siRNA-NC groups were significantly higher, whilst the levels of p-AKT/AKT and p-PI3K/PI3K were significantly decreased (Fig. 10). Compared with that in the PA group, the expression of PEPCK and SOCS3 in the PA + siRNA-NONMMUT031874.2 and PA + MET groups were significantly decreased, whilst the levels of p-AKT/AKT and p-PI3K/PI3K were significantly increased (Fig. 10). In addition, compared with that in the PA + siRNA-NONMMUT031874.2 group, the expression of PEPCK was markedly decreased in the PA + MET group though these differences did not reach statistical significance (Fig. 10F). The expression of SOCS3 in the PA + MET group was decreased significantly compared with that in the PA + siRNA-NONMMUT031874.2 group, although there were no significant differences in the expression of AKT and PI3K among the groups (Fig. 10B and C). These results suggest that the mechanism by which MET improves insulin resistance may be associated with the downregulation of NONMMUT031874.2.

Discussion

Over the past number of decades, the incidence of type 2 diabetes has been consistently increasing. It is expected to increase further by 55% in the year 2035 and affect 591.9 million people globally (25). The pathogenesis of type 2 diabetes is complex. However, the most significant pathogenic

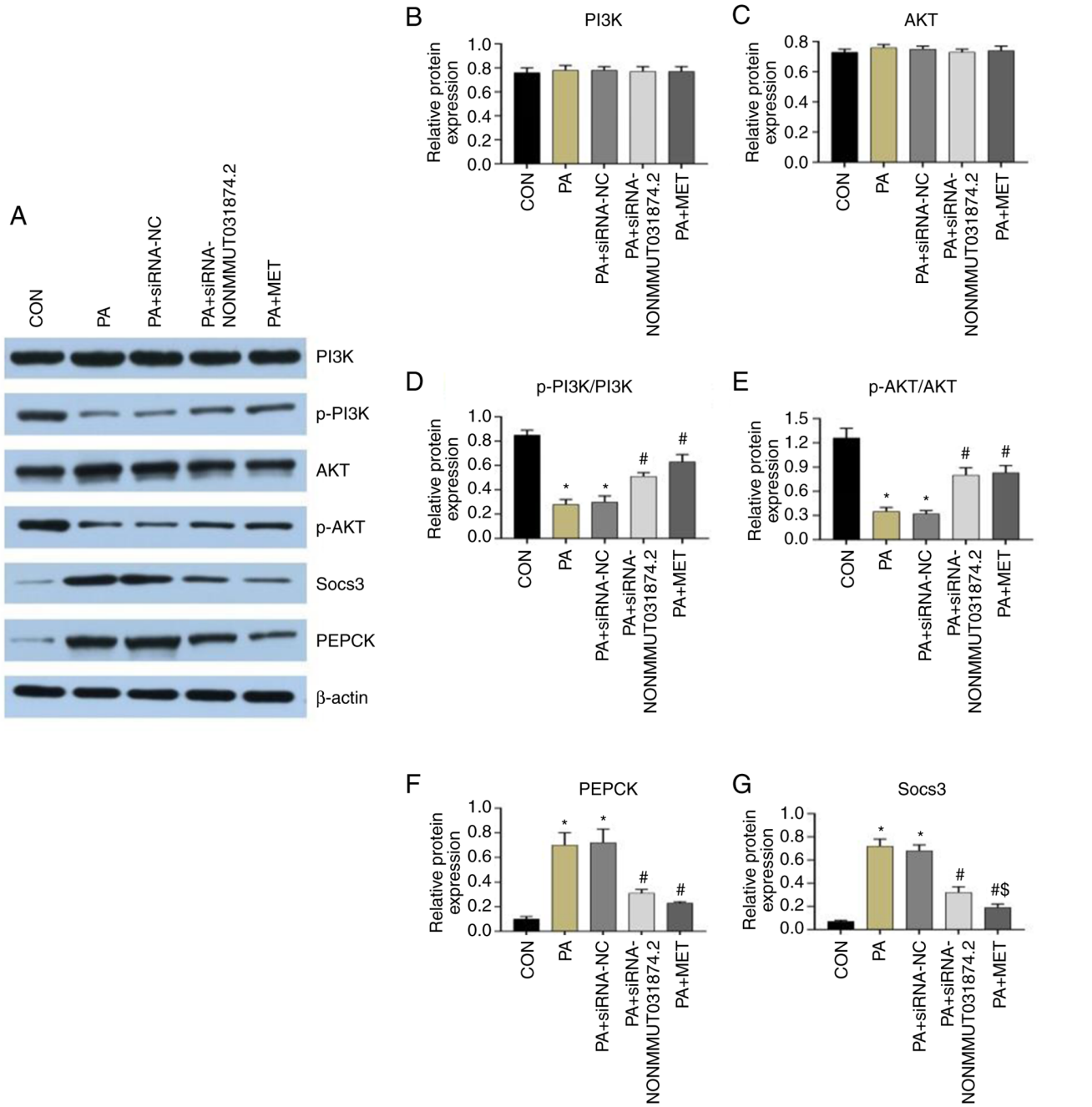

Figure 10. Effect of MET treatment or NONMMUT031874.2 knockdown on insulin signaling. (A) Representative western blotting images insulin signaling pathway components. (B) PI3K, (C) AKT, (D) p-PI3K/PI3K, (E) p-AKT/AKT, (F) PEPCK and (G) Socs3 protein levels. Data are presented as the mean ± SD (n=3). *P<0.05 vs. CON and #P<0.05 vs. PA, $P<0.05 vs. PA + siRNA-NONMMUT031874.2. CON, control; PA, palmitic acid; siRNA, small interfering RNA; NC, negative control; MET, metformin; p-, phosphorylated; Socs3, suppressor of cytokine signaling 3; PEPCK, phosphoenolpyruvate carboxykinase.

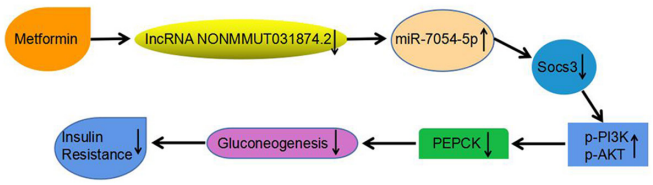

Figure 11. Schematic model of the metformin mechanism according to data in the present study. MET can improve insulin resistance by downregulating the expression of NONMMUT031874.2, increasing the expression of miR-7054-5p and then downregulating the expression of Socs3, which increased the expression of p-PI3K/p-AKT. Socs3, Suppressor of cytokine signaling 3; PEPCK, Phosphoenolpyruvate carboxykinase; lncRNA, long non-coding RNA; microRNA; p-, phosphorylated.

factor is disruption of the insulin signaling pathway, which leads to insulin resistance (26).

Previous studies have shown that lncRNA MALAT1 and NONMMUT008655.2 can promote insulin resistance (27,28). Islet-enriched lncRNA glucose transporter 1 has been reported to be involved in the regulation of insulin secretion. Yin *et al* (29) revealed that downregulation of lncRNA TUG1 can increase islet β cell apoptosis and reduce insulin secretion both *in vitro* and *in vivo* conditions and then regulate the occurrence and development of diabetes. In addition, studies have previously shown that MET can ameliorate insulin resistance in hepatic cells (19) and can exert anti-inflammatory

and antioxidant effects in insulin-resistant HepG2 cells (30). MET also can reduce blood lipid levels and alleviate insulin resistance in mice (31). In the present study, MET significantly reduced fasting blood glucose and insulin levels, in addition to TG, TC and FFA in mice that were fed on a high-fat diet. MET also increased the levels of HDL-C and QUICKI values. These results suggest that MET can reduce insulin resistance in mice fed on a high-fat diet. However, whether MET can improve insulin resistance by regulating the expression of lncRNAs remains controversial.

According to high-throughput sequencing results in the present study, among the upregulated lncRNAs in the HFD group, 386 lncRNAs were downregulated in the HFD + MET group. Among the lncRNAs downregulated in the HFD group, 202 lncRNAs were upregulated in the HFD + MET group. RT-qPCR verified these results, suggesting that MET may improve insulin resistance in mice by regulating the expression of lncRNAs. Among the verified lncRNAs, NONMMUT031874.2 was the most highly expressed. Furthermore, differentially-expressed mRNAs were found to be associated with the insulin signaling pathway, where subsequent pathway analysis predicted that NONMMUT031874.2 was closely related to SOCS3.

SOCS3 is an important member of the SOCS family, which serves as a negative modulator of insulin signaling in sensitive tissues, including hepatocytes and adipocytes (32). In a previous study, it was found that insulin resistance in diabetic mice was significantly improved after knocking down SOCS3 expression. In addition, the expression of SOCS3 in obese mice with insulin resistance is higher compared with that in the control group (33).

The PI3K/AKT pathway is an important component of the insulin signaling pathway that can regulate hepatic glucose synthesis and transport (34). Insulin promotes insulin receptor substrate (IRS) 2 tyrosine phosphorylation and transmits signals through to the PI3K/AKT pathway (35). Previous studies found that in AML12 cells treated with PA, the phosphorylation levels of STAT3 and SOCS3 expression were increased significantly, thereby activating sterol regulatory element binding protein-1c and inhibiting the PI3K/AKT pathway, leading to disorders in glucose and lipid metabolism (36). MET has been found to downregulate the expression levels of PEPCK and G6PC in insulin-resistant HepG2 cells by upregulating the expression levels of IRS-1, p-PI3K and p-AKT (37). Additionally, the levels of inflammatory factors SOCS3, IL-6 and TNF-α were found to be increased in rats fed on an HFD combined with low-dose levostreptozotocin treatment, by acting on the PI3K/AKT pathway to increase blood glucose levels (38). The present study found that, the expression levels of SOCS3, PEPCK and G6PC were increased in the HFD group compared with CON group. After intervention with MET, these changes were reversed. This suggests that MET can reduce insulin resistance.

AML12 cells have been previously used to establish an insulin resistance model *in vitro* (39). In the present study, these cells were treated with 0.25 mM PA to induce insulin resistance, following which glucose concentration in the medium was determined at 0, 8, 16 and 24 h. The glucose concentration in the media was increased at 24 h, suggesting that the insulin resistance model was successfully established.

Previous studies have revealed an increasing number of lncRNAs that can serve important roles in alleviating insulin resistance (40,41). To clarify the potential relationship between NONMMUT031874.2 and SOCS3 further, a lncRNA-miRNA-mRNA network diagram was constructed. According to the NONCODE, miRbase and Targetscan databases, NONMMUT031874.2 and miR-7054-5p; and miR-7054-5p and Socs3 base-pairing diagrams, were created. The results from these diagrams suggest that NONMMUT031874.2 may regulate the expression of SOCS3 through miR-7054-5p. Fan *et al* (42) demonstrated that lncRNA ADAMTS9-AS1 can participate in breast cancer by regulating the expression of miRNA-182 targets. In addition, Zhu *et al* (43) have found that MEG3 can promote hepatic insulin resistance by serving as a ceRNA of miR-214 to facilitate ATF4 expression. However, in HFD fed mice, MEG3 knockdown can upregulate miR-214 expression, downregulate ATF4 expression and then improve insulin resistance.

To explore the function of NONMMUT031874.2, siRNA was used for transfection into AML12 cells to knock down NONMMUT031874.2 expression, before PA and MET were performed. Subsequently, the expression levels of NONMMUT031874.2, miR-7054-5p and insulin signaling pathway-related proteins, in addition to glucose concentration in the culture medium, were all measured in the different groups. The results revealed that knocking down NONMMUT031874.2 expression and treatment with MET mediated similar effects in ameliorating insulin resistance and decreasing the glucose concentrations. In these cells, MET increased the expression of miR-7054-5p by downregulating the expression of NONMMUT031874.2, thereby improving insulin resistance by downregulating the expression of SOCS3, which increased the expression of p-PI3K/p-AKT (Fig. 11).

In conclusion, according to the results of high-throughput sequencing analysis and studies *in vivo* and *in vitro* in the present study, NONMMUT031874.2 appeared to be a key molecule that can alleviate insulin resistance in the liver. These results also suggest that NONMMUT031874.2 may improve insulin resistance through the miR-7054-5p/SOCS3 axis, in addition to being a target of MET for insulin resistance.

Acknowledgements

Not applicable.

Funding

The present study was supported by a Natural Science Foundation of Hebei Province grant (grant no. H201830-7071).

Availability of data and materials

The datasets generated and/or analyzed during the current study are available in the GEO database under the accession number GSE137840.

Authors' contributions

ZMZ performed the experiments, analyzed the data and wrote the manuscript. CW and GYS designed the study and edited

drafts of the manuscript. LLY interpretated the data and revised the manuscript. XMZ and LQY collected the data. ZHL and QN performed the experiments and prepared the figures. ZMZ and ZHL confirm the authenticity of all the raw data. All authors read and approved the final manuscript, and agree to be accountable for all aspects of the work.

Ethics approval and consent to participate

Experiments were approved by the Ethics Committee of Hebei General Hospital (approval no. 2019E368; Shijiazhuang, China) and complied with the Animal (Scientific Procedures) Act 1986 and associated guidelines (14).

Patient consent for publication

Not applicable.

Competing interests

The authors declare that they have no competing interests.

References

1. Ning G: Decade in review-type 2 diabetes mellitus: At the centre of things. Nat Rev Endocrinol 11: 636-638, 2015.
2. Ogurtsova K, da Rocha Fernandes JD, Huang Y, Linnenkamp U, Guariguata L, Cho NH, Cavan D, Shaw JE and Makaroff LE: IDF diabetes atlas: Global estimates for the prevalence of diabetes for 2015 and 2040. Diabetes Res Clin Pract 128: 40-50, 2017.
3. Akash MSH, Rehman K and Liaqat A: Tumor necrosis factor-alpha: Role in development of insulin resistance and pathogenesis of type 2 diabetes mellitus. J Cell Biochem 119: 105-110, 2018.
4. Kurokawa R, Rosenfeld MG and Glass CK: Transcriptional regulation through noncoding RNAs and epigenetic modifications. RNA Biol 6: 233-236, 2009.
5. Ravasi T, Suzuki H, Pang KC, Katayama S, Furuno M, Okunishi R, Fukuda S, Ru K, Frith MC, Gongora MM, *et al*: Experimental validation of the regulated expression of large numbers of non-coding RNAs from the mouse genome. Genome Res 16: 11-19, 2006.
6. Sathishkumar C, Prabu P, Mohan V and Balasubramanyam M: Linking a role of lncRNAs (long non-coding RNAs) with insulin resistance, accelerated senescence, and inflammation in patients with type 2 diabetes. Hum Genomics 12: 41, 2018.
7. Hanson A, Wilhelmsen D and DiStefano JK: The role of long non-coding RNAs (lncRNAs) in the development and progression of fibrosis associated with nonalcoholic fatty liver disease (NAFLD). Noncoding RNA 4: 18, 2018.
8. Pielok A and Marycz K: Non-coding RNAs as potential novel biomarkers for early diagnosis of hepatic insulin resistance. Int J Mol Sci 21: 4182, 2020.
9. Davies MJ, D'Alessio DA, Fradkin J, Kernan WN, Mathieu C, Mingrone G, Rossing P, Tsapas A, Wexler DJ and Buse JB: Management of hyperglycaemia in type 2 diabetes, 2018. A consensus report by the American diabetes association (ADA) and the European association for the study of diabetes (EASD). Diabetologia 61: 2461-2498, 2018.
10. Hundal RS, Krssak M, Dufour S, Laurent D, Lebon V, Chandramouli V, Inzucchi SE, Schumann WC, Petersen KF, Landau BR and Shulman GI: Mechanism by which metformin reduces glucose production in type 2 diabetes. Diabetes 49: 2063-2069, 2000.
11. Ren GF, Xiao LL, Ma XJ, Yan YS and Jiao PF: Metformin decreases insulin resistance in type 1 diabetes through regulating p53 and RAP2A in vitro and in vivo. Drug Des Devel Ther 14: 2381-2392, 2020.
12. Grycel S, Markowski AR, Hady HR, Zabielski P, Kojtallmierska M, Górski J and Blachnio-Zabielska AU: Metformin treatment affects adipocytokine secretion and lipid composition in adipose tissues of diet-induced insulin-resistant rats. Nutrition 63-64: 126-133, 2019.
13. Wang Y, Tang H, Ji X, Zhang Y, Xu W, Yang X, Deng R, Liu Y, Li F, Wang X and Zhou L: Expression profile analysis of long non-coding RNAs involved in the metformin-inhibited gluconeogenesis of primary mouse hepatocytes. Int J Mol Med 41: 302-310, 2018.
14. Ferdowsian H: Human and animal research guidelines: Aligning ethical constructs with new scientific developments. Bioethics 25: 472-478, 2011.
15. Zhao H, Zhang Y, Shu L, Song G and Ma H: Resveratrol reduces liver endoplasmic reticulum stress and improves insulin sensitivity in vivo and in vitro. Drug Des Devel Ther 13: 1473-1485, 2019.
16. Katz A, Nambi SS, Mather K, Baron AD, Follmann DA, Sullivan G and Quon MJ: Quantitative insulin sensitivity check index: A simple, accurate method for assessing insulin sensitivity in humans. J Clin Endocrinol Metab 85: 2402-2410, 2000.
17. Fang F, Li H, Qin T, Li M and Ma S: Thymol improves high-fat diet-induced cognitive deficits in mice via ameliorating brain insulin resistance and upregulating NRF2/HO-1 pathway. Metab Brain Dis 32: 385-393, 2017.
18. Zhang R, Chu K, Zhao N, Wu J, Ma L, Zhu C, Chen X, Wei G and Liao M: Corilagin alleviates nonalcoholic fatty liver disease in high-fat diet-induced C57BL/6 mice by ameliorating oxidative stress and restoring autophagic flux. Front Pharmacol 10: 1693, 2020.
19. Villalva-Pérez JM, Ramírez-Vargas MA, Serafín-Fabían JI, Ramírez M, Moreno-Godínez ME, Espinoza-Rojo M and Flores-Alfaro E: Characterization of Huh7 cells after the induction of insulin resistance and post-treatment with metformin. Cytotechnology 72: 499-511, 2020.
20. Livak KJ and Schmittgen TD: Analysis of relative gene expression data using real-time quantitative PCR and the 2(-delta C(T)) method. Methods 25: 402-408, 2001.
21. Robinson MD, McCarthy DJ and Smyth GK: edgeR: A bioconductor package for differential expression analysis of digital gene expression data. Bioinformatics 26: 139-140, 2010.
22. Moriya Y, Itoh M, Okuda S, Yoshizawa A and Kanehisa M: KAAS: An automatic genome annotation and pathway reconstruction server. Nucleic Acids Res 35 (Web Server Issue): W182-W185, 2007.
23. Rice P, Longden I and Bleasby A: EMBOSS: The European molecular biology open software suite. Trends Genet 16: 276-277, 2000.
24. Li YC, Kang L, Huang J, Zhang J, Liu C and Shen W: Effects of miR-152-mediated targeting of SOCS3 on hepatic insulin resistance in gestational diabetes mellitus mice. Am J Med Sci 361: 365-374, 2021.
25. Guariguata L, Whiting DR, Hambleton I, Beagley J, Linnenkamp U and Shaw JE: Global estimates of diabetes prevalence for 2013 and projections for 2035. Diabetes Res Clin Pract 103: 137-149, 2014.
26. Kim J, Bilder D and Neufeld TP: Mechanical stress regulates insulin sensitivity through integrin-dependent control of insulin receptor localization. Genes Dev 32: 156-164, 2018.
27. Yan C, Chen J and Chen N: Long noncoding RNA MALAT1 promotes hepatic steatosis and insulin resistance by increasing nuclear SREBP-1c protein stability. Sci Rep 6: 22640, 2016.
28. Shu L, Hou G, Zhao H, Huang W, Song G and Ma H: Resveratrol improves high-fat diet-induced insulin resistance in mice by downregulating the lncRNA NONMMUT008655.2. Am J Transl Res 12: 1-18, 2020.
29. Yin DD, Zhang EB, You LH, Wang N, Wang LT, Jin FY, Zhu YN, Cao LH, Yuan QX, De W and Tang W: Downregulation of lncRNA TUG1 affects apoptosis and insulin secretion in mouse pancreatic β cells. Cell Physiol Biochem 35: 1892-1904, 2015.
30. Yang Q, Zhu Z, Wang L, Xia H, Mao J, Wu J, Kato K, Li H, Zhang J, Yamanaka K and An Y: The protective effect of silk fibroin on high glucose induced insulin resistance in HepG2 cells. Environ Toxicol Pharmacol 69: 66-71, 2019.
31. Choi BR, Kim HJ, Lee YJ and Ku SK: Anti-diabetic obesity effects of Wasabia japonica matsum leaf extract on 45% kcal high-fat diet-fed mice. Nutrients 12: 2837, 2020.
32. Cao L, Wang Z and Wan W: Suppressor of cytokine signaling 3: Emerging role linking central insulin resistance and Alzheimer's disease. Front Neurosci 12: 417, 2018.
33. Galic S, Sachithanandan N, Kay TW and Steinberg GR: Suppressor of cytokine signalling (SOCS) proteins as guardians of inflammatory responses critical for regulating insulin sensitivity. Biochem J 461: 177-188, 2014.
34. Song C, Liu D, Yang S, Cheng L, Xing E and Chen Z: Sericin enhances the insulin-PI3K/AKT signaling pathway in the liver of a type 2 diabetes rat model. Exp Ther Med 16: 3345-3352, 2018.

35. Yang P, Liang Y, Luo Y, Li Z, Wen Y, Shen J, Li R, Zheng H, Gu HF and Xia N: Liraglutide ameliorates nonalcoholic fatty liver disease in diabetic mice via the IRS2/PI3K/Akt signaling pathway. Diabetes Metab Syndr Obes 12: 1013-1021, 2019.
36. Xu L, Li Y, Yin L, Qi Y, Sun H, Sun P, Xu M, Tang Z and Peng J: miR-125a-5p ameliorates hepatic glycolipid metabolism disorder in type 2 diabetes mellitus through targeting of STAT3. Theranostics 8: 5593-5609, 2018.
37. Yang Z, Huang W, Zhang J, Xie M and Wang X: Baicalein improves glucose metabolism in insulin resistant HepG2 cells. Eur J Pharmacol 854: 187-193, 2019.
38. Cui X, Qian DW, Jiang S, Shang EX, Zhu ZH and Duan JA: Scutellariae radix and coptidis rhizoma improve glucose and lipid metabolism in T2DM rats via regulation of the metabolic profiling and MAPK/PI3K/Akt signaling pathway. Int J Mol Sci 19: 3634, 2018.
39. Ma H, Yuan J, Ma J, Ding J, Lin W, Wang X, Zhang M, Sun Y, Wu R, Liu C, *et al*: BMP7 improves insulin signal transduction in the liver via inhibition of mitogen-activated protein kinases. J Endocrinol 243: 97-110, 2019.
40. Han M, You L, Wu Y, Gu N, Wang Y, Feng X, Xiang L, Chen Y, Zeng Y and Zhong T: RNA-sequencing analysis reveals the potential contribution of lncRNAs in palmitic acid-induced insulin resistance of skeletal muscle cells. Biosci Rep 40: BSR20192523, 2020.
41. Chen DL, Shen DY, Han CK and Tian Y: LncRNA MEG3 aggravates palmitate-induced insulin resistance by regulating miR-185-5p/Egr2 axis in hepatic cells. Eur Rev Med Pharmacol Sci 23: 5456-5467, 2019.
42. Fan CN, Ma L and Liu N: Systematic analysis of lncRNA-miRNA-mRNA competing endogenous RNA network identifies four-lncRNA signature as a prognostic biomarker for breast cancer. J Transl Med 16: 264, 2018.
43. Zhu X, Li H, Wu Y, Zhou J, Yang G and Wang W: lncRNA MEG3 promotes hepatic insulin resistance by serving as a competing endogenous RNA of miR-214 to regulate ATF4 expression. Int J Mol Med 43: 345-357, 2019.